

# Extracellular vesicles from human plasma dampen inflammation and promote tissue repair functions in macrophages

Alan M. Adamczyk<sup>1</sup> | María Luz Leicaj<sup>1</sup> | Martina Paula Fabiano<sup>1</sup> | Gonzalo Cabrerizo<sup>1</sup> |  
Nadia Bannoud<sup>2</sup> | Diego O. Croci<sup>2</sup> | Kenneth W. Witwer<sup>3,4</sup> | Federico Remes Lenicov<sup>1</sup> |  
Matías Ostrowski<sup>1</sup> | Paula Soledad Pérez<sup>1</sup>

<sup>1</sup>Instituto de Investigaciones Biomédicas en Retrovirus y SIDA (INBIRS), Universidad de Buenos Aires-CONICET, Buenos Aires, Argentina

<sup>2</sup>Laboratorio de Glicobiología y Biología Vascular, Instituto de Histología y Embriología de Mendoza, CONICET-Universidad Nacional de Cuyo, Mendoza, Argentina

<sup>3</sup>Department of Molecular and Comparative Pathobiology, The Johns Hopkins University School of Medicine, Baltimore, Maryland, USA

<sup>4</sup>Department of Neurology, The Johns Hopkins University School of Medicine, Baltimore, Maryland, USA

#### Correspondence:

Paula Soledad Pérez  
Email: [psperez@ffyba.uba.ar](mailto:psperez@ffyba.uba.ar)

Matías Ostrowski  
Email: [maostro@fmed.uba.ar](mailto:maostro@fmed.uba.ar)

#### Funding information

Argentinean National Agency for Science and Technology Promotion (ANPCYT), Grant/Award Numbers: PICT 2015-00658, PICT 2019-00907, PICT-2018-02202, PICT-2019-02506; United States National Institutes of Health, National Institute on Drug Abuse, Grant/Award Number: R01DA040385; University of Miami Center for AIDS Research/Sylvester Comprehensive Cancer Center Argentina Consortium for AIDS-Malignancies, Grant/Award Number: U54-CA0221208

#### Abstract

Although inflammation is a vital defence response to infection, if left uncontrolled, it can lead to pathology. Macrophages are critical players both in driving the inflammatory response and in the subsequent events required for restoring tissue homeostasis. Extracellular vesicles (EVs) are membrane-enclosed structures released by cells that mediate intercellular communication and are present in all biological fluids, including blood. Herein, we show that extracellular vesicles from plasma (pEVs) play a relevant role in the control of inflammation by counteracting PAMP-induced macrophage activation. Indeed, pEV-treatment of macrophages simultaneously with or prior to PAMP exposure reduced the secretion of pro-inflammatory IL-6 and TNF- $\alpha$  and increased IL-10 response. This anti-inflammatory activity was associated with the promotion of tissue-repair functions in macrophages, characterized by augmented efferocytosis and pro-angiogenic capacity, and increased expression of VEGFa, CD300e, RGS2 and CD93, genes involved in cell growth and tissue remodelling. We also show that simultaneous stimulation of macrophages with a PAMP and pEVs promoted COX2 expression and CREB phosphorylation as well as the accumulation of higher concentrations of PGE2 in cell culture supernatants. Remarkably, the anti-inflammatory activity of pEVs was abolished if cells were treated with a pharmacological inhibitor of COX2, indicating that pEV-mediated induction of COX2 is critical for the pEV-mediated inhibition of inflammation. Finally, we show that pEVs added to monocytes prior to their M-CSF-induced differentiation to macrophages increased efferocytosis and diminished pro-inflammatory cytokine responses to PAMP stimulation. In conclusion, our results suggest that pEVs are endogenous homeostatic modulators of macrophages, activating the PGE2/CREB pathway, decreasing the production of inflammatory cytokines and promoting tissue repair functions.

#### KEYWORDS

CREB, exosomes, extracellular vesicles, human plasma, infection, inflammation, macrophages, PGE2, resolution, tissue homeostasis, wound-healing

Alan M. Adamczyk and María Luz Leicaj contributed equally to this work.

This is an open access article under the terms of the [Creative Commons Attribution-NonCommercial-NoDerivs License](https://creativecommons.org/licenses/by-nc-nd/4.0/), which permits use and distribution in any medium, provided the original work is properly cited, the use is non-commercial and no modifications or adaptations are made.

© 2023 The Authors. *Journal of Extracellular Vesicles* published by Wiley Periodicals, LLC on behalf of the International Society for Extracellular Vesicles.

## 1 | INTRODUCTION

Acute inflammation is a defence response to infection initiated immediately upon pathogen recognition and is vital to eradicating threats to the organism. This response is coordinated by several families of pro-inflammatory factors, including cytokines, chemokines and lipid mediators (such as prostaglandins and leukotrienes) which induce an increase in vascular permeability and orchestrate leukocyte recruitment. Increased vascular permeability allows passage of plasma to the interstitium and generation of oedema. Macrophages are key players during inflammation, being essential for the effective control and clearance of viral, bacterial, fungal and protozoal infections. One of their primary functions after pathogen encounter is the promotion of an inflammatory response, mainly through the secretion of pro-inflammatory mediators such as cytokines interleukin (IL)-1 $\beta$ , IL-6, IL-12, IL-18, IL-23 and tumour necrosis factor-alpha (TNF- $\alpha$ ) (Hamidzadeh et al., 2017). These inflammatory anti-microbial macrophages are known as classically activated or M1 macrophages (Mosser & Edwards, 2008; Murray, 2017). Since uncontrolled or persistent inflammation can lead to pathology (Nathan & Ding, 2010), an active and coordinated program of inflammation resolution initiates shortly after the inflammatory response begins (Serhan & Savill, 2005). The resolution phase of inflammation is associated with the acquisition of anti-inflammatory and tissue repair functions by macrophages, which characterize a different effector phenotype, usually named as alternatively activated or M2-like macrophage (Locati et al., 2020; Murray, 2017). This reparative response is mediated by an array of anti-inflammatory (i.e., IL-10) and pro-resolution factors (i.e., resolvins, maresins, lipoxins, among others) (Basil & Levy, 2016), many of which are secreted by M2-like macrophages. In addition, effective resolution of inflammation depends on efferocytosis, the mechanism whereby macrophages remove apoptotic cells (mainly granulocytes recruited to the inflammatory foci) (Dalli & Serhan, 2012 Oct 11). Efferocytosis is also an important trigger for macrophage switch from inflammatory (M1) to tissue-repair (M2-like) phenotype (Serhan & Savill, 2005) with further production of pro-resolution mediators (Freire-De-Lima et al., 2006). Finally, macrophages also produce growth factors and mediators that promote angiogenesis (Vannella & Wynn, 2017). Therefore, macrophages are key actors not only in driving the inflammatory response needed to contain the infection but also in the subsequent events required for controlling the initial response and restoring tissue homeostasis (Vannella & Wynn, 2017).

Among the factors that regulate the macrophage transition from inflammation to resolution is prostaglandin E2 (PGE2), the most abundant prostaglandin in humans (Serhan & Levy, 2003). While PGE2 can act as a pro-inflammatory factor during the early stages of the response (Nakayama et al., 2006; Wang & Lau, 2006; Weller et al., 2007; Yu & Chadee, 1998), it switches to anti-inflammatory functions in later phases (Kalinski, 2012; Scher & Pillinger, 2009). PGE2 is the main product of cyclooxygenases in myeloid and stromal cells. In tissues, levels of this prostaglandin are regulated by the local balance between prostaglandin G/H synthase 2 (PTGS2 or COX2)-driven synthesis and 15-hydroxyprostaglandin-dehydrogenase mediated degradation (Phipps et al., 1991; Tai et al., 2002). In conjunction with TLR stimulation, PGE2 suppresses IL-12 and TNF- $\alpha$  production and partially suppresses IL-6 production in macrophages (Kuroda & Yamashita, 2022). Moreover, PGE2 increases IL-10 release from macrophages in a PKA-dependent manner (Mackenzie et al., 2013). Finally, PGE2 suppresses inflammasome activation, attenuating the release of IL-1 $\beta$  (Sokolowska et al., 2015), and stimulates polarization of macrophages to a M2-like phenotype via the cyclic AMP-responsive element binding (CREB)-mediated induction of Kruppel-like factor 4 (Luan et al., 2015).

Extracellular vesicles (EVs) are a heterogeneous group of membrane-delimited structures released by cells. EVs mediate the intercellular delivery of proteins, lipids and nucleic acids contained on the surface or within the EV lumen (Théry et al., 2009), modifying the function of recipient cells (Colombo et al., 2014; Théry et al., 2009). EVs are found in many biological fluids, including blood (Karimi et al., 2018), where their concentration reportedly increases in diseases such as cancer (Khan et al., 2014; Rabinowits et al., 2009; Taylor & Gercel-Taylor, 2008), HIV infection (Pérez et al., 2019) and inflammatory conditions (Buzas et al., 2014). Elegant studies performed in zebrafish demonstrated that patrolling macrophages are major contributors to the uptake of both endogenous and exogenously administered EVs (Hyenne et al., 2019; Verweij et al., 2019). In concordance, chemical depletion of monocytes and macrophages in mice dramatically increases the stability of circulating EVs (Imai et al., 2015). Moreover, it has been shown that circulating tumour EVs are able to transform the phenotypes of macrophages in vivo (Plebanek et al., 2017). Although the molecular determinants of the interaction between plasma EVs and macrophages are unknown, different reports have shown specific ligand/receptor interactions promoting uptake of EVs by macrophages (Atay et al., 2011; Barrès et al., 2010; Feng et al., 2010; Yuyama et al., 2012). Thus, it appears that macrophages are preferred targets for circulating EVs. Along these lines, circulating EVs from different pathological conditions have been shown to interact with macrophages and contribute to inflammation (Hu et al., 2021). However, the homeostatic role of EVs present in the plasma of healthy individuals in the control of inflammatory responses is less characterized.

Previous reports have shown that the endothelium of vessels present in solid tumours and at sites of inflammation exhibits increased leakiness, forming gaps that range from 0.2 to 1.4  $\mu$ m (Baluk et al., 1997; Hirata et al., 1995). These endothelial gaps, together with dilatation of the vessels are responsible for generating an increase in vascular permeability that allows the passage of nanometer-sized particles (including EVs and synthetic nanoparticles in the range of 100 nm) into tumours and/or inflamed or injured tissues. For instance, mesenchymal stem cell (MSC)-derived EVs have been shown to accumulate preferentially into the kidneys of mice with acute kidney injury but not of control mice (Grange et al., 2014). Likewise, EV-based nanoparticles, polymer

nanoparticles and liposomes inoculated into mice accumulate at inflamed sites due to changes in the vasculature (Brusini et al., 2020; Liu et al., 2020; Yan et al., 2020). Based on these studies, we hypothesize that plasma EVs would access acutely inflamed tissues as part of the plasma exudate generated due to an increase in endothelial permeability, and that they would interact with macrophages modulating their response to microbial pathogen-associated molecular patterns (PAMPs). Thus, in this study, we evaluated the ability of purified human plasma EVs (pEV) to modulate macrophage activation following exposure to different microbial PAMPs.

## 2 | RESULTS

### 2.1 | pEVs inhibit inflammatory response to PAMPs

Plasma EVs were obtained from blood of fasted healthy donors by size exclusion chromatography (SEC) followed by centrifugation at  $30,000 \times g$  for 90 min and resuspension in phosphate-buffered saline (PBS) (Figure 1a). Centrifugation of pEV-enriched SEC fractions at  $30,000 \times g$  for 90 min was validated by Western blotting (WB) to be sufficient to pellet most pEVs in the sample, equivalent to centrifugation at  $100,000 \times g$  (Figure S1a). pEV characterization was performed in compliance with the MISEV 2018 guidelines (Théry et al., 2018). Firstly, immunoblot analysis showed that pEV preparations were enriched in the canonical EV markers CD63, CD81 and CD9 (transmembrane) as well as ALIX and HSP70 (cytosolic), as compared with plasma (Figure 1b,c). Conversely, IgG and albumin, two of the most abundant plasma proteins, were depleted from the pEV fractions (Figure 1b–d). Additionally, APOA1, a protein characteristic of high-density lipoproteins (HDL), and APOB-100, a protein enriched in low-density and very-low-density lipoproteins (LDL and VLDL) were also shown to be depleted from the pEV fractions (Figure 1b,c). Thus, purity assessment indicated that our pEV preparations were not significantly contaminated with either soluble or other particulate plasma components. Transmission electron microscopy (TEM) visualization revealed that pEVs had the expected lipid bilayer-membrane and (artefactual) cup-shaped morphology (Figure 1e) with a median (IQR 25%–75%) diameter of 142.0 (111.5–175.5) nm (Figure 1f). pEVs were further characterized by particle analysis platforms: nanoparticle-tracking analysis (NTA) (Figure 1g,h) and microfluidic resistive pulse sensing (MRPS) (Figure S1b,c). Consistent with TEM data, particle analysis of pEVs showed a size distribution compatible with small extracellular vesicles, such as exosomes and small microvesicles (Figure 1g, Figure S1b). The pEV population detected by NTA had a mean diameter of  $199.0 \pm 6.6$  nm and a mode diameter of  $146.5 \pm 7.0$  nm. The concentration of isolated pEVs as calculated for the original plasma sample was  $2.4 \pm 0.6 \times 10^8$  EVs/mL (NTA determination, Figure 1h), in accordance with data reported for circulating EVs in healthy individuals (Karimi et al., 2022).

To analyse the effect of plasma EVs on macrophage functionality, we selected an *in vitro* model of blood monocyte-derived macrophages (MDMs). Monocytes were obtained from blood of volunteer healthy donors and differentiated to macrophages for 7 days with macrophage-colony stimulating factor (M-CSF, 50 ng/mL). Cells were then exposed to the toll-like receptor (TLR) 7/8 agonist Resiquimod (RSQ) or the TLR4 agonist lipopolysaccharide (LPS) in the presence or absence of freshly purified pEVs. As an additional control, cells were stimulated with pEVs alone. After 24 h, cytokines IL-6, TNF- $\alpha$  and IL-10 were measured in cell culture supernatants, and cell viability was analysed to confirm that neither PAMP nor pEV treatment induced cell mortality (Figure S2a). Whereas stimulation with either RSQ or LPS triggered the release of IL-6, TNF- $\alpha$  and IL-10, pEVs alone induced significant secretion of neither the pro-inflammatory cytokines IL-6 and TNF- $\alpha$  nor the anti-inflammatory IL-10 (Figure S2b). Interestingly, when macrophages were simultaneously exposed to either RSQ or LPS and pEVs, secretion of IL-6 and TNF- $\alpha$  was reduced, whereas secretion of IL-10 was augmented (Figure 2a,b). Similar results were obtained by exposing macrophages to autologous pEVs (Figure S2c). As expected, the modulatory effect of pEVs on cytokine secretion followed a dose-dependent response (Figure 2c). Paralleling the analysis of secreted cytokines, qPCR analysis showed downregulation of mRNA of IL-6 and TNF- $\alpha$  and upregulation of IL-10 mRNA at 4 h post-stimuli (Figure 2d).

To better understand the dynamics of pEV inhibition of macrophage inflammation, we evaluated the effect of asynchronous PAMP and pEV stimulation. Pre-treatment of MDMs with pEVs up to 24 h before PAMP exposure and simultaneous stimulation with PAMP + pEVs inhibited IL-6 production (Figure 2e) both for RSQ and LPS. Strikingly, when pEVs were added after PAMP, the inhibitory effect mediated by pEVs was seen only if they were added soon after RSQ stimulation (1 h) and not after more extended times of RSQ pre-treatment (4 and 6 h), while it was not observed for LPS.

To verify the specificity of the effect mediated by pEVs on macrophages, we first performed an additional step of purification of pEVs by performing an iodixanol density cushion (IDC) before SEC separation to obtain highly pure pEVs (Karimi et al., 2018). These pEVs were also very efficient at inhibiting inflammation in MDMs (Figure S2D–F). Next, to analyse whether the anti-inflammatory effect mediated by pEVs on macrophages was specific for EVs from this source, we evaluated the anti-inflammatory activity of EVs produced by two cell lines. Results show that in contrast to pEVs, EVs produced by the human embryonic kidney 293T (HEK293T) and the CD4+ T cell leukaemia Jurkat cell lines triggered rather than suppressed inflammation (Figure S2g). Finally, we corroborated that the anti-inflammatory effect was not a consequence of PAMP binding to pEVs; for that, we measured LPS using LAL reagent on pEVs incubated with this PAMP and washed afterwards, showing that there was no detection of

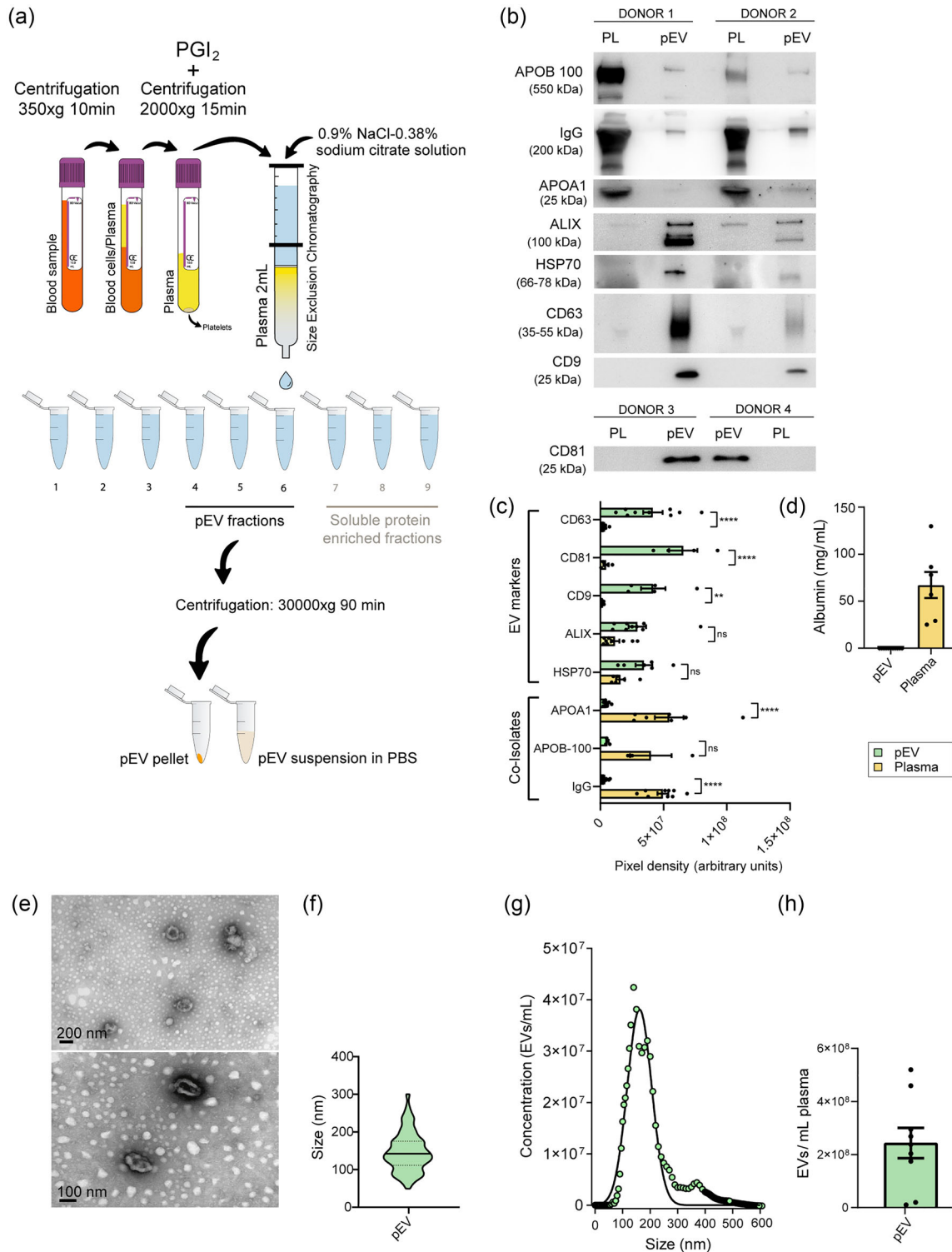


**FIGURE 1** Obtention and characterization of plasma EVs. (a) Plasma from fasted healthy donors was recovered after sequential centrifugation with addition of 200 nM prostaglandin I<sub>2</sub> (PGI<sub>2</sub>) to inhibit platelet activation. Plasma EVs (pEV) were isolated from 2 mL of plasma by size exclusion chromatography (SEC). pEV-containing 1-mL fractions (numbered 4–6) were combined, concentrated by centrifugation at 30,000 × g, and resuspended in PBS for characterization and biological experiments. (b) Immunoblot characterization of pEVs from individual donors with antibodies directed against the EV markers CD63, CD81, CD9, Alix and HSP70 and the non-EV markers IgG, APOA1 and APOB-100. Plasma was loaded as a positive control for non-EV co-isolates. (c) Pixel density quantifications from immunoblots corresponding to  $n = 3–9$  pEV preparations with antibodies directed against the EV markers CD63, CD81, CD9, Alix and HSP70 and the non-EV markers IgG, APOA1 and APOB-100 (mean ± SEM) (d) Albumin in pEV preparations from individual donors ( $n = 6$ ) was quantified by immunoturbidimetry (mean ± SEM). (e) TEM visualization of pEVs purified by SEC combined with centrifugation at 30,000 × g, as depicted in (a). Scale bars in nm are shown for both micrographs in the lower left corner. (f) Violin plot showing median pEV diameter measured in TEM micrographs using Image J software, on a total of 137 EV-compatible structures observed. (g) Size distribution of pEVs from individual donors ( $n = 9$ )

(Continues)



**FIGURE 1** (Continued)

obtained by NTA, showing mean concentration for each EV size (green circles) and the non-linear regression fit (line). (h) Concentration of pEVs (mean  $\pm$  SEM) isolated by SEC followed by centrifugation, determined by NTA ( $n = 9$ ). (\*\* $p < 0.01$ ; \*\*\*\* $p < 0.0001$ ; ns = not significant).

residual LPS on pEVs (data not shown). Hence, we conclude that not all EVs are naturally anti-inflammatory and that it is unlikely that the effect herein described for pEVs is due to plasma contaminants nor to quenching of PAMP by pEVs.

Overall, these results demonstrate that pEVs have an anti-inflammatory effect on macrophages exposed to a viral or bacterial PAMP, characterized by reduced IL-6 and TNF- $\alpha$  and increased IL-10 secretion.

## 2.2 | pEVs promote tissue repair functions in macrophages

To assess whether pEVs could promote tissue repair functions in macrophages, we first analysed by qPCR the expression of a set of genes involved in cell growth and tissue remodelling (Hamidzadeh et al., 2020). Of note, transcripts for VEGFa, CD300e, CD93 and RGS2 were significantly upregulated in RSQ + pEV-treated MDMs compared with RSQ treatment alone at 4 h post-stimuli (Figure 3a). In contrast, pEVs as a single stimulus did not modulate the expression of the mentioned genes. To further characterize the phenotype of MDMs simultaneously exposed to RSQ + pEV, we analysed their capacity to phagocytose apoptotic cells. This process, known as efferocytosis, is a central macrophage function needed for inflammation resolution. pEV treatment significantly increased efferocytosis capacity of RSQ-exposed MDMs compared with RSQ alone (Figure 3b). Finally, we explored the pro-angiogenic capacity of macrophages, which is a critical process of their tissue-repair potential during the resolution phase of inflammatory response. Concordantly with gene expression data, RSQ + pEV-treated macrophages secreted higher amounts of VEGF (Figure 3c). Thus, to functionally evaluate whether macrophage stimulation with pEVs modulated the angiogenic process, we performed an in vitro assay of tube formation of human umbilical vein endothelial cells (HUVEC). We observed that conditioned media from pEV-stimulated macrophages induced robust in vitro angiogenesis, even when compared with RSQ treatment alone (Figure 3d). These data indicate that pEVs not only dampen inflammatory responses of macrophages exposed to a PAMP, but also promote efferocytosis and pro-angiogenic activities.

## 2.3 | pEVs favour monocyte differentiation towards macrophages with decreased inflammatory and enhanced tissue-repair functions

At the site of infection, blood monocytes are recruited and differentiated into macrophages in response to cytokines and other factors present in the local microenvironment. To investigate whether pEVs could enhance monocyte differentiation towards a M2-like profile, monocytes were differentiated into macrophages with M-CSF for 5 days in the presence or absence of pEVs. M-CSF-differentiated macrophages have a M2-like basal phenotype characterized by the surface expression of markers associated with endocytic and phagocytic processes typical of resolution of inflammation, such as CD163, CD206 and merTK. Addition of pEVs further increased the expression of these molecules (Figure 4a) as well as that of major histocompatibility complex II (MHC II) molecules. To confirm the anti-inflammatory phenotype of these macrophages, we evaluated cytokine response to PAMP stimulation and macrophage efferocytosis capacity. Macrophages differentiated from monocytes exposed to pEVs at day 0 were stimulated after 5 days with either RSQ or LPS and cytokine secretion was quantified in 24-h cell culture supernatants. We observed that macrophages obtained from pEV-treated monocytes produced reduced amounts of IL-6 and TNF- $\alpha$  while secreting higher levels of IL-10, as compared with macrophages obtained from untreated monocytes (Figure 4b). Finally, we observed that pEV-treatment of monocytes also resulted in macrophages that exhibited greater efferocytosis capacity (Figure 4c). These results indicate that pEVs favour polarization of monocytes towards macrophages with reduced inflammatory and enhanced tissue-repair functions.

## 2.4 | The inhibitory effect of pEVs on macrophages is mediated by PGE2 production

Previous studies have shown that PGE2 directs the transition of LPS-treated MDMs from an inflammatory towards a growth-promoting phenotype (Hamidzadeh et al., 2020). pEV-treated MDMs exposed to RSQ resembled the transitional wound-healing phenotype mediated by PGE2 in LPS-stimulated macrophages. Therefore, we wondered whether PGE2 could be involved in the anti-inflammatory and wound-healing phenotype promoted by pEVs. PGE2 levels were evaluated by a homogeneous time-resolved fluorescence competitive assay in 24 h supernatants of MDMs treated with RSQ in the presence or absence of pEVs. Results showed a higher concentration of PGE2 released by pEV-treated MDMs compared with RSQ treatment alone (Figure 5a), indicating a pEV-induced production of this prostaglandin. In contrast, pEV treatment alone did not induce PGE2 synthesis.

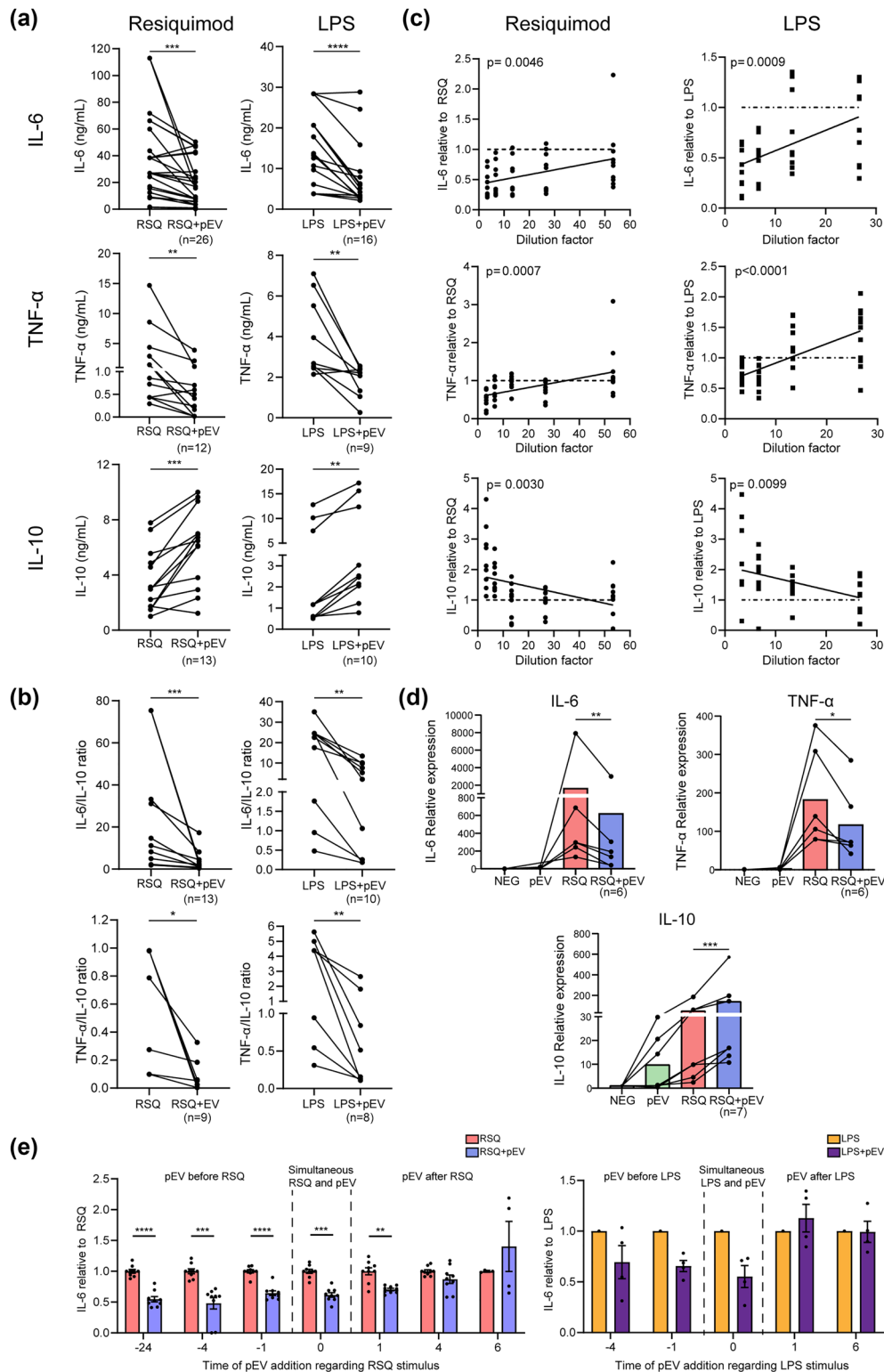


**FIGURE 2** Plasma EVs inhibit macrophage inflammatory response to RSQ and LPS. Isolated pEVs from individual donors were used to treat MDMs differentiated for 7 days with M-CSF and exposed or not to RSQ (0.5  $\mu$ g/mL) or LPS (1 ng/mL). Cytokine secretion into cell culture supernatant was measured by ELISA or CBA at 24 h post-stimulation. Cytokine gene expression was also evaluated by qPCR at 4 h post-stimulation. (a) Cytokine secretion by MDMs simultaneously stimulated with pEV and RSQ (left column) or pEV and LPS (right column), as compared to PAMP stimulation alone. The number of individual pEV donors stimulated with pEVs and either RSQ or LPS, respectively is: 16 and 5 for IL-6; 9 and 3 for TNF- $\alpha$ ; 11 and 3 for IL-10. (b) IL-6 to IL-10 and TNF- $\alpha$  to IL-10 secretion ratios in RSQ or LPS-exposed MDMs treated or not with pEVs. The number of individual pEV donors analysed is indicated in each graph. The number of independent MDMs stimulated with pEVs and either RSQ or LPS, respectively is: 11 and 3 for IL-6/IL-10 ratio; 6 and 3 for TNF- $\alpha$  to IL-10 ratio. (c) Cytokine secretion by MDMs simultaneously stimulated with RSQ or LPS

(Continues)

**FIGURE 2** (Continued)

and decreasing doses of pEV from individual donors ( $n = 10$ ), relative to PAMP stimulation alone (dashed lines); data from two independent experiments and statistical significance for the linear regressions are shown. (d) Relative IL-6, TNF- $\alpha$  and IL-10 gene expression levels in MDMs treated with pEV alone or in combination with RSQ versus unstimulated (NEG) and RSQ only treatment. The number of pEV preparations (obtained from plasma pooled from 3 to 4 donors) analysed is indicated in each graph. The number of independent MDMs stimulated with pEVs is  $n = 4$  for IL-6;  $n = 5$  for TNF- $\alpha$  and  $n = 5$  for IL-10. (e) MDMs were treated with pEV either before ( $-24$  h,  $-4$  h and  $-1$  h), simultaneously (0 h) or after (1 h, 4 h, 6 h) RSQ (left panel) or LPS (right panel) stimulation. The concentration of IL-6 secreted into cell culture supernatant by cells stimulated with PAMP only or PAMP + pEV was determined at 24 h after PAMP stimulation. Graphs show the combination of two independent MDM donors including  $n = 9$  pEV donors for RSQ and  $n = 4$  pEV donors for LPS, expressing IL-6 concentration in the PAMP + pEV condition relative to PAMP treatment alone. ( $*p < 0.05$ ;  $**p < 0.01$ ;  $***p < 0.001$ ;  $****p < 0.0001$ ).

COX2 was found to be significantly upregulated in the RSQ + pEV condition (Figure 5b). This enzyme is the primary cyclooxygenase controlling PGE2 synthesis in response to inflammation (Murakami et al., 2000), and its upregulation could explain the increased PGE2 production in macrophages treated with RSQ + pEV.

In order to better understand the contribution of endogenous COX2-derived PGE2 to the decreased activation phenotype of pEV-treated macrophages exposed to RSQ, the activity of COX2 was pharmacologically inhibited by treating cells with the selective inhibitor Celecoxib (Cib). Afterwards, macrophages were stimulated with RSQ alone or in combination with pEVs, and TNF- $\alpha$  secretion into the supernatant was evaluated 4 h later by ELISA. Celecoxib treatment did not alter the response to RSQ (data not shown). In agreement with results shown in Figure 2a, pEV treatment inhibited TNF- $\alpha$  secretion in RSQ-treated macrophages. Remarkably, in macrophages pre-treated with Cib, the anti-inflammatory action of pEV was decreased (Figure 5c). These results suggest that COX2-induced prostaglandin production is involved in pEV-dampening of the inflammatory response to RSQ. Since PGE2 induces its own production (Kalinski, 2012), we wondered whether the observed PGE2 increment could be attributed to PGE2 present on pEVs. Measurements of PGE2 on pEV-preparations showed that this prostaglandin was indeed detected, with a mean  $\pm$  SEM concentration of  $64.7 \pm 10.0$  pg/mL. Whether pEV-associated PGE2 is responsible for triggering *de novo* PGE2 production in macrophages will be the subject of future studies.

To further characterize the cellular pathways involved in the pEV-induced acquisition of a tissue-repair (M2-like) phenotype, we analysed the phosphorylation status of CREB, a key transcription factor involved in dampening macrophage inflammatory response (Na et al., 2015; Ruffell et al., 2009). Immunoblot analysis showed that when macrophages were treated with RSQ alone, the amount of phosphorylated CREB (pCREB) peaked at 5 min post-stimulus and rapidly decayed to levels around those of the untreated control (Figure 5d,e). Strikingly, when macrophages were treated with RSQ in the presence of pEVs, the amount of pCREB continued to rise up to levels twice as high as those obtained with RSQ alone, peaking at 40 min post-stimuli (Figure 5d,e). These results suggest that pEVs activate the cyclic adenosine monophosphate (cAMP)/protein kinase A (PKA)/CREB pathway, and that this modulation is enhanced in an inflammatory setting upon PAMP recognition.

Altogether, these results support the hypothesis that pEVs activate the cAMP/PKA/CREB pathway in macrophages exposed to RSQ, leading to COX2 induction and further PGE2 production, which, ultimately, could be responsible for dampening inflammatory response and promoting transition to a tissue-repair (M2-like) phenotype (Figure 5f).

### 3 | DISCUSSION

Macrophages detect and respond to aggressions from the outside, participating in the initiation and maintenance of inflammation. Because failure to stop and resolve inflammation can lead to tissue damage and pathology, macrophages also possess a myriad of mechanisms to dampen inflammatory responses and to restore tissue homeostasis. Herein, we demonstrate that EVs circulating in the plasma of healthy individuals contribute to the control of macrophage activation induced by different microbial PAMPs by reducing the production of pro-inflammatory cytokines and concurrently promoting the acquisition of tissue repair functions.

The presence of EVs in blood plasma was reported decades ago (Crawford, 1971; George et al., 1982). Numerous studies have proposed the use of circulating EVs as biomarkers of diseases (Hoshino et al., 2020; Kalani et al., 2020; Quinn et al., 2015; Vacchi et al., 2020). Regarding their functionality, it has been suggested that circulating EVs mediate intercellular communication between different cell types throughout the body. For instance, it has been shown that plasma EVs mediate the intertissue communication of eNAMPT, a critical enzyme of the NAD<sup>+</sup> biogenesis pathway, thus contributing to the maintenance of NAD<sup>+</sup> homeostasis and delaying aging (Yoshida et al., 2019). Other studies have shown that physical exercise triggers the release of EVs into circulation (Brahmer et al., 2019; Frühbeis et al., 2015; Just et al., 2020; Oliveira et al., 2018), contributing to skeletal muscle adaptations to training (Just et al., 2020; Oliveira et al., 2018). Furthermore, exercise-derived EVs have also been implicated in cardioprotection in different experimental settings (Bei et al., 2017; Hou et al., 2019). In addition to participating in physiology and homeostasis, circulating EVs can play a pathogenic role by fuelling immune cell activation in inflammatory diseases, such as ulcerative colitis (Hu et al., 2021; Liu et al., 2018; Wong et al., 2016), acute pancreatitis (Bonjoch et al., 2016) and sepsis (Masironi et al., 2011). Finally, we and others have shown that circulating EVs from HIV-infected individuals promote macrophage

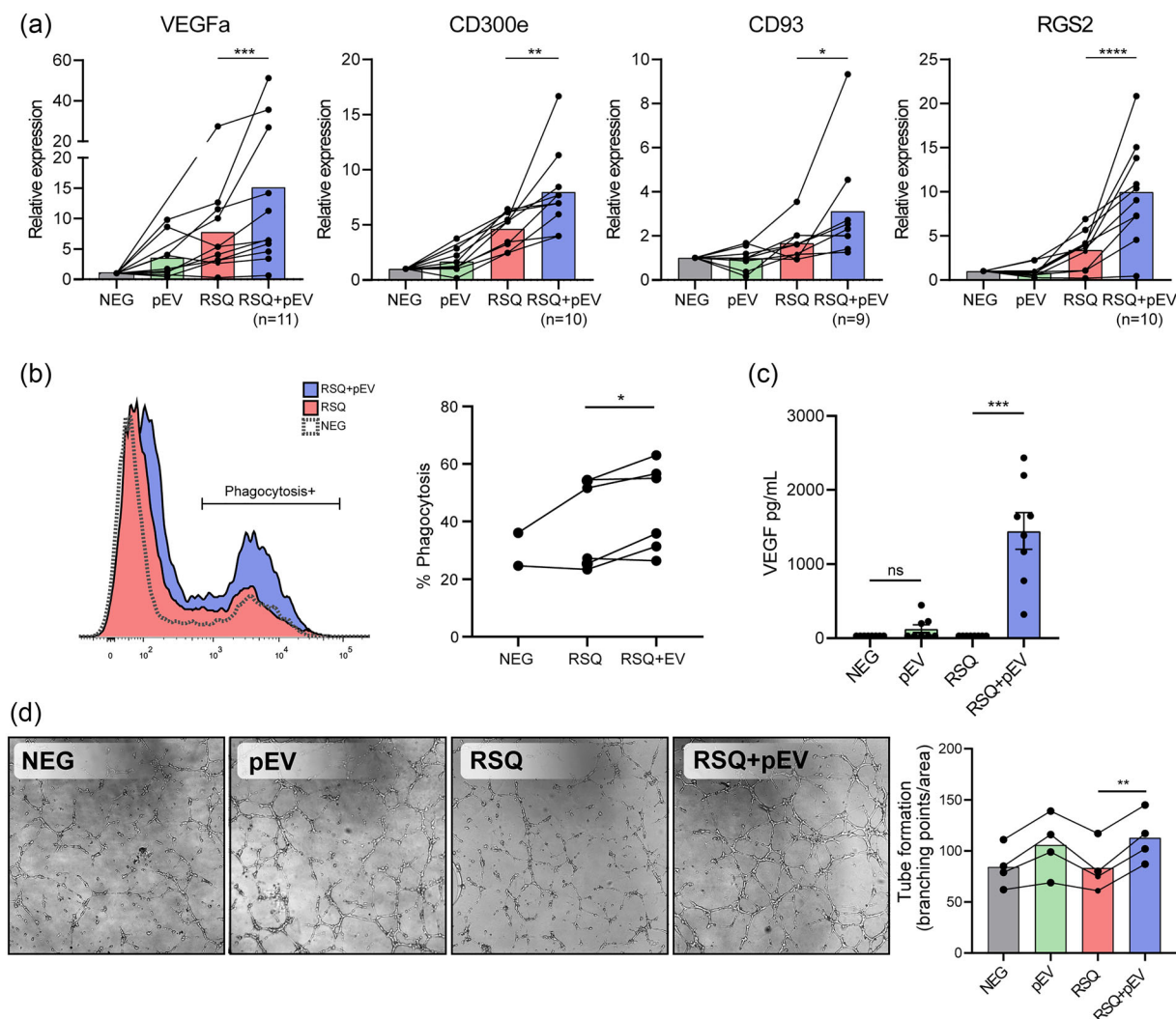


**FIGURE 3** Plasma EVs promote tissue-repair functions in macrophages exposed to RSQ. (a) Quantitative RT-PCR of genes involved in tissue repair and angiogenesis (VEGFa, CD300e, CD93 and RGS2) evaluated at 4 h in RNA of MDMs exposed to the different experimental conditions. Relative expression levels were normalized to housekeeping gene GAPDH and to unstimulated condition (NEG). The number of pEV preparations (obtained from plasma pooled from 3 to 4 donors) analysed is indicated in each graph. The number of independent MDMs stimulated with pEVs is  $n = 9$  for VEGFa, 5 for CD300e, 7 for CD93 and 8 for RGS2. Statistical comparison between RSQ versus RSQ + pEV conditions was performed by ratio paired *t* test. (b) Phagocytosis of apoptotic cells. MDMs untreated (NEG) or treated with RSQ or RSQ + pEV for 24 h were trypsinised and mixed with CFSE-labelled apoptotic Jurkat cells (1:2) in 1% FBS-RPMI. After 1 h incubation at 37°C, phagocytosis was stopped by washing with cold PBS. Cells were maintained in ice until cytometric acquisition. Left: a representative histogram showing the phagocytosis positive population. Right: Quantification of phagocytosis percentages in two independent MDM cultures stimulated with pEVs from six individual donors. (c) VEGF secretion by MDMs treated with pEVs alone or in combination with RSQ versus unstimulated (NEG) and RSQ only treatment, measured by ELISA 24-h post-stimulation. Eight independent MDM cultures each treated with a single pEV donor are shown. (d) Tube formation assay. Starved HUVEC ( $n = 2$ ) were stimulated with conditioned media from MDMs treated with the experimental conditions (corresponding to 4 independent MDM cultures each with a single pEV donor) in a 1:2 dilution and incubated at 37°C for 6 h. Representative photographs taken for each condition are shown. Tube formation was quantified by counting the number of branching points in the total photographed area. (\* $p < 0.05$ ; \*\* $p < 0.01$ ; \*\*\* $p < 0.001$ ; \*\*\*\* $p < 0.0001$ ).

activation and the release of inflammatory cytokines (Bernard et al., 2014; Chettimada et al., 2018; Duette et al., 2018; Ostalecki et al., 2016). Thus, depending on their origin and the pathophysiological context, EVs present in circulation can promote or inhibit inflammation. Remarkably, previous studies have shown that exogenously administered “healthy” EVs are able to reach and infiltrate inflamed tissues (Deng et al., 2013; Escobar et al., 2020; French et al., 2020; Nakazaki et al., 2021). Indeed, it is likely that the entry of EVs into inflamed tissues occurs during the period of increased vascular permeability that takes place during inflammatory processes, as previously reported for other nanoparticles (Brusini et al., 2020; Liu et al., 2020; Yan et al., 2020). In this scenario, we hypothesize that in healthy individuals with a local inflammatory reaction, plasma EVs reach inflamed tissues as part of the inflammatory exudate. After extravasation, pEVs interact with macrophages, tuning their control of the inflammatory process.



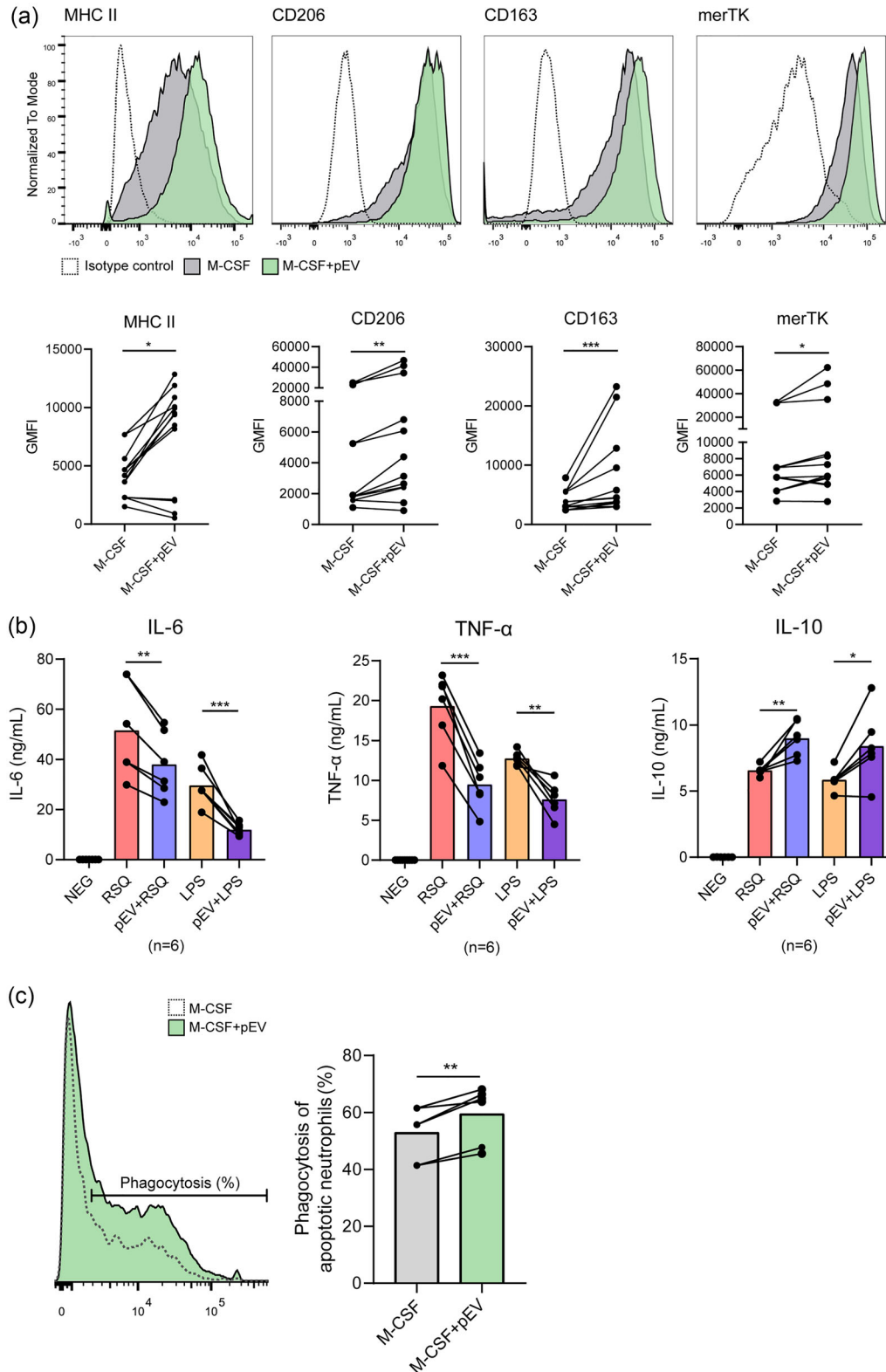


**FIGURE 4** Plasma EVs favour monocyte differentiation towards macrophages with decreased inflammatory and enhanced tissue-repair functions. Monocytes were differentiated with M-CSF (50 ng/mL) in the presence or absence of pEVs for 5 days. (a, upper panel) Representative histograms showing MHC-II, CD206, CD163 and merTK expression of pEV-treated cells (green) compared to no-EV control (grey), and isotype control (dotted line) analysed by flow cytometry. (A, lower panel) Summary of 7 independent MDM cultures stimulated with pEVs from 13 individual donors, (mean  $\pm$  SEM) showing geometric mean fluorescence intensities (GMFI) of the mentioned markers in the pEV-treated condition compared with the non-EV control (M-CSF differentiation alone). (b) Cytokine profile on 24-h supernatants of MDMs ( $n = 2$  independent cultures) differentiated in the presence or absence of pEVs ( $n = 6$  individual donors) for 5 days and further stimulated with RSQ or LPS (c) Phagocytosis of apoptotic cells. MDMs differentiated with M-CSF at 50 ng/mL alone or in combination with pEVs were trypsinised at day 5 and mixed with CFSE-labelled apoptotic neutrophils (1:2) in FBS 1%-RPMI. After 1 h incubation at

(Continues)

FIGURE 4 (Continued)

37°C, phagocytosis was stopped by washing with cold PBS. Cells were maintained on ice until cytometric acquisition. Left: Representative histograms showing the phagocytosis-positive population. Right: Quantification of phagocytosis in three independent macrophages stimulated with pEVs from six individual donors. (\* $p < 0.05$ ; \*\* $p < 0.01$ ; \*\*\* $p < 0.001$ ).

EVs are considered to exert their functions as intercellular messengers by mediating the cytoplasmic delivery of molecules (i.e., RNAs) to recipient cells or by stimulating a cell membrane receptor with a ligand (i.e., a protein) present on the EV surface (Théry et al., 2009). Regarding their role in macrophage polarization, both EV-mediated transfer of miRNAs (Cooks et al., 2018; Park et al., 2019; Qian et al., 2020) and EV surface expression of growth factors (Tkach et al., 2022) have been implicated. Although we do not yet know the EV cargo molecule(s) responsible for inducing the modulation of macrophage phenotype, we found that pEVs mediate the induction of PGE2 production by macrophages. This prostaglandin is, in turn, critical for the anti-inflammatory activity of pEVs. Indeed, inhibition of PGE2 production by pharmacological blockade of macrophage COX2 prevented pEVs from controlling inflammation. Thus, although more investigation is needed to elucidate the complex mechanism underlying pEV-mediated modulation, our data suggest that induction of the PGE2 pathway is involved.

PGE2 is a local mediator that can be produced by all cell types, but epithelia, fibroblasts and infiltrating inflammatory cells, such as monocytes and macrophages, are major sources of PGE2 in inflammatory foci (Kalinski, 2012). PGE2 exerts its functions mainly in an autocrine and paracrine fashion, acting on macrophages through two Gs-coupled receptors, EP2 and EP4, and triggering the cAMP/PKA/CREB pathway (Fujino et al., 2005; Honda et al., 1993; Regan et al., 1994). This signalling pathway mediates the dominant aspects of the anti-inflammatory and suppressive activity of PGE2, including induction of anti-inflammatory gene expression (Na et al., 2015) and suppression of pro-inflammatory cytokines and chemokines' response to LPS (Gill et al., 2016; Takayama et al., 2002). In addition to promoting the control of inflammation, recent work published by Hamidzadeh et al. (2020) demonstrated that PGE2 also promotes transition of LPS-stimulated M-CSF macrophages to a growth-promoting and pro-angiogenic phenotype, characterized by upregulated expression of VEGFa, CD300e, RGS2 and CD93, among other signature genes, and acquisition of tissue repair activities. Our results show that plasma EV treatment recapitulates most of the effects on macrophages that Hamidzadeh and collaborators assigned to PGE2, including the expression of a set of growth-promoting genes, reduction of pro-inflammatory cytokine production and enhanced pro-resolution functions. The ability of EVs to induce PGE2 production by EV-recipient macrophages has been previously demonstrated for both tumour and MSC-derived EVs (Hyvärinen et al., 2018; Linton et al., 2018). However, to the best of our knowledge, this is the first report describing PGE2 induction by EVs isolated from plasma. Although the mechanisms underlying the EV-mediated induction of PGE2 and other eicosanoids are not clear, it has been shown that eicosanoids and the enzymes in charge of their synthesis are present in EVs (Boilard, 2018; Deng et al., 2013; Duchez et al., 2015; Rossaint et al., 2016; Subra et al., 2010; Xiang et al., 2009). Since detectable levels of PGE2 were found on pEVs, we hypothesize that pEV-PGE2 could serve as a trigger for endogenous PGE2 production, as this prostaglandin is shown to autoamplify by inducing COX2 (Cho & Choe, 2020; Hsu et al., 2017; Suda et al., 1998), and thus lead to the acquisition of anti-inflammatory and tissue-repair functions in macrophages. Furthermore, it has been proposed that EV-associated miRNAs can regulate PGE2-levels (Donzelli et al., 2021). Investigating how plasma EVs boost PGE2 production by macrophages will be an important subject of future research.

It is noteworthy that pEV treatment in the presence of a TLR7/8 agonist promoted rapid CREB phosphorylation and at higher levels than those observed for the agonist alone (Figure 5d,e). Transcription factor CREB is phosphorylated on Ser-133 in response to an array of stimuli and has well known roles in cell proliferation, differentiation, and survival (Shaywitz & Greenberg, 1999), along with functions in immunity (Wen et al., 2010). In particular, it has been shown that CREB is phosphorylated following PGE2 stimulation of macrophages in a cAMP/PKA dependent fashion, participating in polarization towards a pro-resolution phenotype (Luan et al., 2015; Na et al., 2015). Considering this background, together with our experimental data showing pEV-mediated induction of PGE2 and CREB phosphorylation, we suggest that pEVs rapidly activate the cAMP/PKA/CREB pathway in macrophages upon contact or internalization, inducing PGE2 production. This, in turn, leads to a positive activation loop of the cAMP/PKA/CREB pathway, responsible for promoting the anti-inflammatory and tissue-repair (M2-like) phenotype (Figure 5f). More research is needed to determine whether PGE2 or other pEV-cargoes trigger this pathway, as well as the receptors involved.

Finally, results in Figure 2e show that pEVs are effective at regulating macrophage inflammation only during the initial phase of the response. In addition, as shown in Figure 4, pEVs also favour polarisation of monocytes towards macrophages with tissue-repair functions and diminished inflammatory response. Altogether, these results indicate that pEVs prime macrophages and monocytes towards an anti-inflammatory and tissue-repair (M2-like) phenotype. Hence, we suggest that by acting on both monocytes and macrophages, pEVs act at the onset of inflammation as a homeostatic mechanism.

Blood derived EVs are being actively investigated for their anti-inflammatory and regenerative properties (De Boer & Davies, 2022; Wu et al., 2021). As an example, in an in vitro co-culture system of primary osteoarthritic chondrocytes and activated M1 macrophages, treatment with blood-products derived EVs reduced TNF- $\alpha$  and IL-1 $\beta$  secretion (Othahal et al., 2021). Another interesting study reported that serum EVs from normal mice but not from fibrotic mice reduced hepatic fibrosis in carbon tetrachloride or thioacetic acid-induced liver injury mice models, also showing reduced levels of inflammatory infiltration and

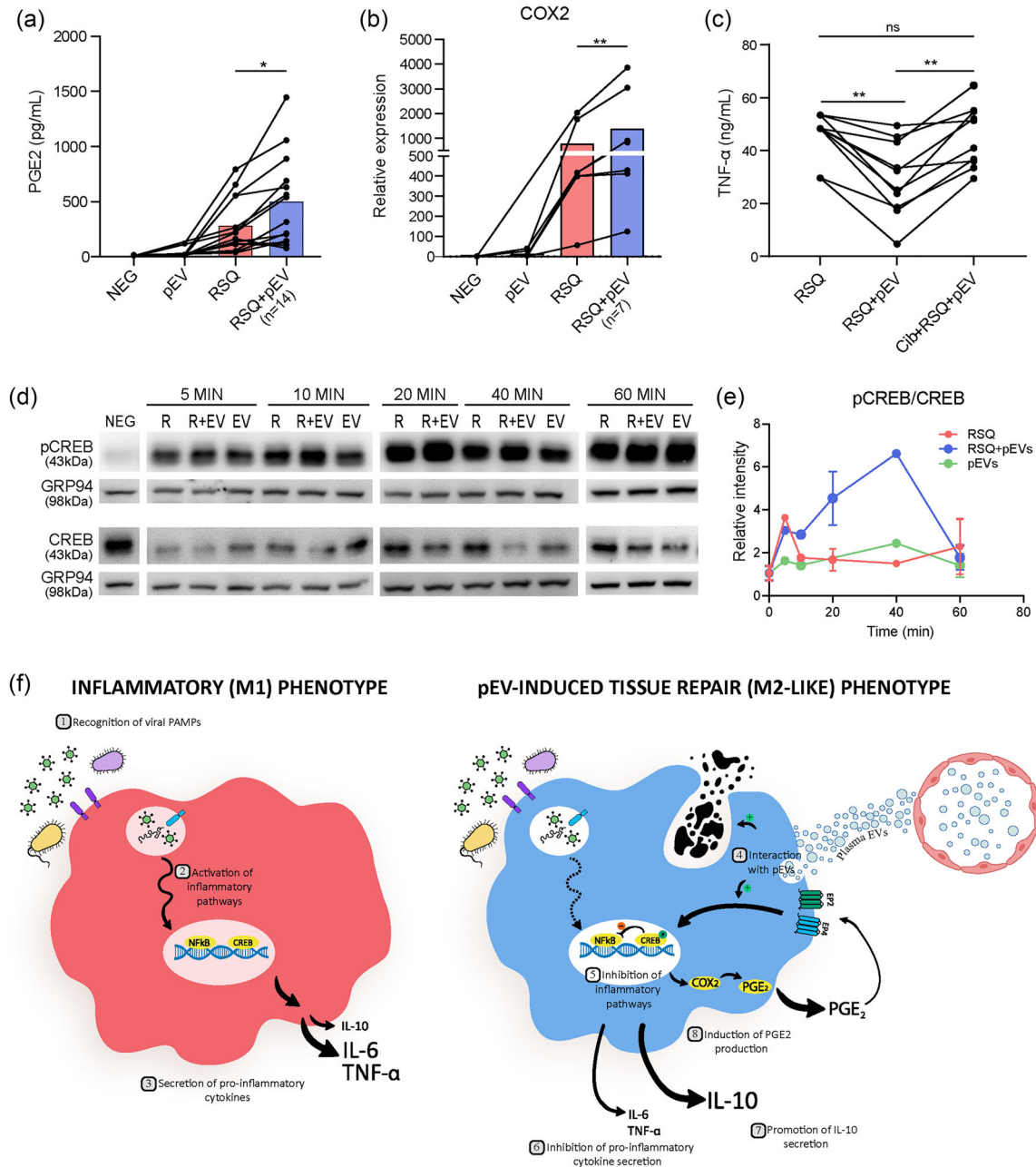


**FIGURE 5** PGE<sub>2</sub> production is involved in pEV-inhibitory effect on macrophages. (a) PGE<sub>2</sub> was evaluated by a homogeneous time-resolved fluorescence competitive assay. PGE<sub>2</sub> concentration on 24 h-supernatants of MDMs treated with pEVs alone or in combination with RSQ versus unstimulated (NEG) and RSQ only treatment is shown. Results from 6 independent MDM cultures stimulated with pEVs from 14 individual donors. (\**p* < 0.05). (b) Relative expression of COX2 at 4 h on MDMs exposed to the different experimental conditions, normalized to housekeeping gene GAPDH and to unstimulated condition (NEG). Results from five independent MDM cultures stimulated with seven pEV preparations (obtained from plasma pooled from 3 to 4 donors) are shown. Statistical comparison between RSQ versus RSQ + pEV conditions was performed by ratio paired *t* test (C) MDMs (three independent donors) pretreated or not for 20 min with 25 μM Celecoxib (Cib) were stimulated with RSQ alone or in combination with pEVs from 2, 5 and 3 individual donors in each experiment; TNF-α secretion into supernatants was evaluated 4 h later by ELISA. (d) Representative immunoblots showing pCREB kinetics on MDMs along time (5, 10, 20, 40 and 60 min) after RSQ treatment (R) in the absence or presence of pEVs (R + EV), or treatment with pEVs alone (EV), versus untreated control (NEG). GRP94 was used as loading control. (e) Kinetics of p-CREB/CREB ratio, measured as band intensity quantification in four independent experiments. (f) Working model. Macrophages exposed to infections detect PAMPs such as single-stranded RNA molecules in the endocytic compartments through TLR7/8 receptors and LPS by TLR4 in plasma membrane (1). This interaction triggers molecular signals leading to NFκB activation (2) and synthesis of pro-inflammatory cytokines (3), typical of inflammatory (M1) macrophages. However, when plasma EVs reach the site of infection, they interact with and/or are uptaken by macrophages (4) and induce sustained CREB phosphorylation. pCREB suppresses NFκB-mediated transcription (5) thus reducing transcription of pro-inflammatory cytokines (6), and induces IL-10 (7) and COX2 transcription, among other genes, with the consequent increase in PGE<sub>2</sub> production (8). PGE<sub>2</sub> acts in an autocrine and paracrine fashion to promote a tissue-repair (M2-like) phenotype in macrophages. Thus, we propose that plasma EVs act as endogenous immunomodulators of macrophages at the site of infection, promoting the transition from inflammation to resolution. (\**p* < 0.05; \*\**p* < 0.01; ns: not significant).

pro-inflammatory cytokines (Chen et al., 2018). Although these studies did not directly address how blood-derived EVs modulate macrophages, they showed reduced inflammation cues. Thus, we consider that the ability of pEVs to dampen macrophage-mediated inflammation reported in this study is responsible, at least in part, for these therapeutic effects of pEVs.

In conclusion, our results reveal plasma EVs as endogenous homeostatic immunomodulators of macrophages and monocytes at the site of infection, enhancing the transition from inflammation to resolution. Further identification of the molecular pEV factors responsible for these anti-inflammatory and tissue-repair functions may lead to the discovery of therapeutic candidates for treating inflammatory conditions with a principal macrophagic component. Ultimately, future investigations in animal models are needed to understand the *in vivo* impact of circulating EVs on inflammation, and, more importantly, the plausible utility of human plasma-derived extracellular vesicles as therapies for inflammatory diseases.

## 4 | MATERIALS AND METHODS

### 4.1 | Plasma samples

Plasma samples for pEV separation were obtained from volunteer fasted healthy donors older than 18 years who had completed and passed a survey on blood donation and were screened for serological markers before being accepted as donors. Blood extraction was performed by venipuncture using EDTA-containing vacutainer tubes (BD Biosciences, San Jose, CA). Plasma was recovered after centrifugation at  $350 \times g$  for 10 min, and then depleted of platelets by centrifugation at  $2000 \times g$  for 15 min with addition of 200 nM prostaglandin I<sub>2</sub> (PGI<sub>2</sub>) (Cayman Chemical, Ann Arbor, MI) to inhibit platelet activation. Finally, aliquots were stored at  $-80^{\circ}\text{C}$  until use.

### 4.2 | Isolation of pEVs by size exclusion chromatography (SEC)

Purification of pEVs was accomplished by size exclusion chromatography following a protocol adapted from Böing et al. (Böing et al., 2014; Duette et al., 2018). Sepharose CL-2B columns (Cytiva, Uppsala, Sweden) were assembled using 12-mL empty cartridges with 20-mm hydrophobic frits (Applied Separations, Allentown, PA). Two millilitres of plasma were loaded on top, and 1-mL fractions were eluted using 0.9% NaCl–0.38% sodium citrate solution. pEV containing fractions (fractions 4–5–6) were centrifuged at  $30,000 \times g$  at  $4^{\circ}\text{C}$  for 90 min in a centrifuge (Biofuge Stratos, rotor Heraeus, k-factor = 340). Pellets were pooled and resuspended in 50  $\mu\text{L}$  of phosphate-buffered saline (PBS).

### 4.3 | Isolation of pEVs by iodixanol density cushion and size-exclusion chromatography (IDC + SEC)

A combination of iodixanol density cushion and SEC was used for isolation of lipoprotein-free pEVs (Karimi et al., 2018). In brief, 6 mL of plasma was layered on top of a 2 mL 50%, 2 mL 30% and 2 mL 10% OptiPrep (Sigma-Aldrich, St. Louis, MO, USA) cushion, and centrifuged at  $178,000 \times g$  (TH-641 rotor, k-factor 133, Sorvall wX+ Ultracentrifuge) for 2 h at  $4^{\circ}\text{C}$ . A visible band between the 10% and 30% layers was collected, brought to 2 mL with PBS, and loaded onto a SEC column and pEVs were purified as described previously.

All relevant data regarding EV-experiments have been submitted to the EV-TRACK knowledgebase (EV-TRACK ID: EV220310) (Van Deun et al., 2017).

### 4.4 | Transmission electron microscopy (TEM)

A droplet of each pEV suspension fixed in 2% paraformaldehyde was mounted on a collodion-coated copper grid (400 mesh) for 20 min. Then, grids were washed three times with PBS (pH 7.4) and once with distilled water. Samples were incubated with 4% uranyl acetate for 40 s for contrast. Finally, grids were visualized under a JEM 1200 EX II transmission electron microscope (JEOL Ltd., Tokyo, Japan) and photographed by an Erlangshen ES1000W camera (Model 785, Gatan Inc., Pleasanton, CA, USA) at the *Electron Microscopy Central Service from University of La Plata, Veterinary Science School* (Servicio Central de Microscopía Electrónica de la Facultad de Ciencias Veterinarias, Universidad de La Plata).

### 4.5 | Nanoparticle-tracking analysis (NTA)

Plasma samples were obtained from EDTA-anticoagulated whole blood venipuncture from nine healthy fasted donors. Plasma EVs were isolated by SEC followed by centrifugation at  $30,000 \times g$  for 90 min as described above and resuspended in PBS. Size



distribution and concentration of pEVs were analysed using NanoSight NS300 equipment (NanoSight, Amesbury, UK). The analysis was performed using a 532 nm laser and 565 nm long pass filter, with a camera level of 12, video time of 30 s, and detection threshold of 5. pEVs were diluted in PBS before the analysis.

#### 4.6 | Microfluidic resistive pulse sensing (MRPS)

Plasma EVs from three healthy donors were isolated by SEC followed by centrifugation at  $30,000 \times g$  for 90 min, as described above. Purified pEVs were resuspended in 50  $\mu\text{L}$  PBS. MRPS measurements were conducted using the nCSI instrument (Spectradyne, Torrance, CA, USA). pEVs were diluted  $10^5$ – $10^7$  times in 0.1% Tween 20-PBS, and 5  $\mu\text{L}$  were loaded onto polydimethylsiloxane cartridges (diameter range 65 nm to 400 nm). About 5000 events were recorded for each sample. Data were analysed using the nCSI Data Analyzer (Spectradyne, Torrance, CA). For all samples, user-defined filtering was applied by defining 2D polygonal boundaries based on transition time and diameter to exclude false positive signals.

#### 4.7 | Culture and differentiation of human monocyte-derived macrophages (MDMs)

Buffy coats from healthy anonymous blood donors were processed by Ficoll-Paque (Cytiva, Uppsala, Sweden) density gradient centrifugation. Peripheral blood mononuclear cells were recovered and monocytes were purified using magnetic CD14+ microbeads by positive selection (Miltenyi Biotec, Germany). Depending on the needs of each experiment, monocytes were cultured in 96, 48, 24 or 12-well plates in RPMI 1640 culture medium (Sigma-Aldrich, St. Louis, MO, USA) supplemented with 10% FBS (Sigma-Aldrich, St. Louis, MO, USA) and 50 ng/mL M-CSF (Miltenyi Biotec) growth factor for 7 days.

#### 4.8 | Cell stimulation

pEV stimulation was always performed as per the following criteria: pEVs obtained from 2 mL of plasma were resuspended in 50  $\mu\text{L}$  PBS and used to treat 500,000 macrophages at a 0.15 dilution (24-well plate). This dose of pEVs was previously determined to be suitable for macrophage stimulation (Duette et al., 2018). For experiments performed in different plate formats with other amounts of cells, pEV-dose was adjusted to maintain the aforementioned ratio of pEVs/cells. Whenever indicated, other dilutions of pEV preparations were used.

TLR7/8 agonist Resiquimod (R848) (Invivogen, San Diego, CA) was used at 0.5  $\mu\text{g}/\text{mL}$  for all experiments. LPS (Sigma-Aldrich, St. Louis, MO) was used at 1 ng/mL. For the COX-2 inhibition experiments, Celecoxib (Cayman Chemical, Ann Arbor, MI) was used at 25  $\mu\text{M}$ .

#### 4.9 | Cytokine measurements

Concentrations of human IL-6, TNF- $\alpha$  and IL-10 were quantified by ELISA (BD Biosciences, San Jose, CA) or by cytokine bead array (CBA) (BD Biosciences, San Jose, CA) according to the manufacturer's instructions. VEGF in supernatants was quantified by a Human VEGF ELISA kit (R&D Systems, Minneapolis, USA) according to the manufacturer's instructions.

#### 4.10 | RNA extraction and qPCR

For expression analyses, stimulated macrophages were lysed at 4 h post-stimuli, after which mRNA extraction was performed using the PureLink RNA mini kit (Invitrogen, Thermo Fisher Scientific, USA) with on-column DNase I treatment (TransGen Biotech, Beijing, China) following manufacturer's instructions. Nucleic acid was eluted in 30  $\mu\text{L}$  elution buffer and stored at  $-80^\circ\text{C}$  until use. Double-stranded cDNA was synthesized with M-MLV reverse transcriptase (Promega, Madison, WI). Quantitative PCR (PRISM 7500; Applied Biosystems, Foster City, CA), was performed using LightCycler 480 SYBR Green I Master mix (Roche, Basel, Switzerland) and primer pairs as listed in Table S1. Cycle thresholds (Ct) were normalized to the Ct of GAPDH, and fold enrichments were calculated compared to the values from unstimulated control cells.

#### 4.11 | Western blotting

Macrophages were lysed with radioimmunoprecipitation assay buffer using phosphatase inhibitor (PhosSTOP, Roche, Basel, Switzerland) and protease inhibitor (Protease Inhibitor Cocktail, Sigma-Aldrich, St. Louis, MO, USA). Protein samples were quantified with Pierce BCA Protein Assay Kit (Thermo Fisher Scientific, Waltham, MA, USA), 15  $\mu\text{g}$  were loaded on

10% SDS-PAGE per condition and transferred to a polyvinylidene difluoride (PVDF) membranes (Immuno-Blot LF PVDF, Bio-Rad, Hercules, CA, USA). After blocking the membranes with 5% non-fat milk in Tris-buffered saline containing 0.05% Tween for 1 h at room temperature, they were incubated with primary antibodies including phospho-serine133 CREB (Cell Signalling Technology, Danvers, MA, USA), total CREB (Cell Signalling Technology, Danvers, MA, USA) and GRP94 (Enzo Life Sciences, Villeurbanne, France) overnight at 4°C.

For EV characterization, pEVs from healthy donors were isolated from 2 mL of plasma according to the above sections. EV-containing 1-mL fractions (Locati et al., 2020; Nathan & Ding, 2010; Serhan & Savill, 2005) were combined, concentrated by centrifugation at  $30,000 \times g$  for 90 min, resuspended in PBS and later lysed in Laemmli buffer. Equal volumes of extracts were separated on 12% SDS-PAGE under non-reducing conditions for CD63, CD9, CD81 and IgG detection, 10% SDS-PAGE under reducing conditions for ALIX, HSP70 and APOA1, and 8% SDS-PAGE under reducing conditions for APOB-100 detection, and further blotted on PVDF transfer membrane. Primary antibodies used were as follows: CD63, clone H5C6 (556019, BD Pharmingen, Franklin Lakes, NJ); CD9, clone M-L13 (555370, BD Pharmingen Franklin Lakes, NJ); CD81, clone JS-81 (555675, BD Pharmingen, Franklin Lakes, NJ); ALIX, clone E6P9B (92880, Cell Signalling Technology, Danvers, MA, USA); HSP70, clone C92F3A-5 (ADI-SPA-810, Enzo Life Sciences, Villeurbanne, France); APOA1, clone 5F4 (3350S, Cell Signalling Technology, Danvers, MA); and APOB-100 (20a-g1B, Academy Bio-Medical, Waltham, MA). Primary antibody dilution used for blotting was 1/10000 for IgG and 1/1000 for the rest of the antibodies. Anti-species secondary antibodies conjugated to HRP were used at 1/10000 dilution. All blots were revealed using SuperSignal West Pico PLUS Chemiluminescent Substrate (Thermo Fisher Scientific, Waltham, MA, USA), and images were acquired with the BioSpectrum-815 Imaging System (UVP, Upland, CA, USA).

#### 4.12 | Flow cytometry

For surface staining, macrophages were trypsinised and resuspended in 2% FBS-PBS. Cells were pretreated with Human Fc Block (BD Pharmingen, Franklin Lakes, NJ) for 10 min before antibody staining for 30 min at 4°C. Antibodies used were: HLA-DR/DQ/DP-FITC, clone REA33 (Miltenyi Biotec); merTK-PECy7, clone 590H11G1E3 (BioLegend, San Diego, CA, USA); CD163-PE, clone GHI/61 (BioLegend, San Diego, CA, USA); CD206-AF647, clone 15-2 (BioLegend, San Diego, CA, USA). Data were acquired on a FACSCanto cytometer (BD Biosciences, San Jose, CA, USA) and analysed using FlowJo X software.

#### 4.13 | Phagocytosis of apoptotic cells

Neutrophils and Jurkat cells were used as apoptotic cells for efferocytosis evaluation. Human neutrophils were prepared by Ficoll-Paque (Cytiva, Uppsala, Sweden) gradient centrifugation and dextran sedimentation, followed by removal of erythrocytes by hypotonic lysis, and left overnight in 5% FBS-RPMI for natural apoptosis to occur. Apoptosis of Jurkat cells was induced with 1 nM staurosporine for 6 h. Apoptotic cells were washed with PBS and labelled with 5  $\mu$ M carboxy-fluorescein diacetate succinimidyl ester (CFSE) (Sigma-Aldrich, St. Louis, MO) for 5 min at 37°C. After labelling, cells were washed with 5% FBS-RPMI and left in medium for 15 min to eliminate leftover CFSE. Finally, cells were resuspended to  $5 \times 10^6$  cells/mL in 1% FBS-RPMI. MDMs were trypsinised and mixed with CFSE-labelled apoptotic cells (1:2) in a final volume of 200  $\mu$ L of 1% FBS-RPMI. After 1 h incubation at 37°C, phagocytosis was stopped by washing with cold PBS. Cells were maintained in ice until cytometric acquisition on a FACSCanto (BD Biosciences, San Jose, CA, USA) cytometer. Analyses were performed using FlowJo X software.

#### 4.14 | Tube formation assay

Primary human umbilical vein endothelial cells (HUVEC) were purified from human umbilical vein as previously reported (Bannoud et al., 2022). For tube formation assays, HUVEC were starved for 2 h in RPMI 1640 without FBS. Afterwards, cells were trypsinised, collected and plated on an angiogenesis micro slide (Ibidi GmbH, Gräfelfing, Germany) at a density of  $1 \times 10^4$  cells per well over 10  $\mu$ L of solidified Geltrex LDEV-free (Gibco). Negative control cells were incubated with serum-free RPMI; positive control cells were exposed to RPMI 15% FBS + 20 ng/mL of human VEGF and the remaining cells were stimulated with conditioned media from macrophages in a 1:2 dilution. Then, the micro slide was incubated at 37°C for 6 h. Finally, the formation of tubular structures in the total area was photographed at a 4 $\times$  magnification by a Nikon Eclipse microscope. Branching points were considered for the count, using the multi-point tool of Image J Software for the analysis.

#### 4.15 | Statistical analyses

Data analysis was performed with GraphPad Prism 8.0 (GraphPad Software, La Jolla, CA, USA). Statistical differences were assessed by paired analysis of variance (ANOVA) or t test. Differences with a *p*-value < 0.05 were considered significant.

## AUTHOR CONTRIBUTIONS

**Alan Adamczyk:** Investigation-Equal. **María Leicaj:** Investigation-Equal; Visualization-Equal. **Martina Fabiano:** Investigation-Equal. **Gonzalo Cabrerizo:** Investigation-Supporting. **Nadia Bannoud:** Investigation-Supporting. **Diego Croci:** Writing – Review & Editing-Supporting. **Kenneth Witwer:** Funding acquisition- Equal; Writing - Review and Editing-Equal. **Federico Remes Lenicov:** Writing – Review & Editing-Equal. **Matías Ostrowski:** Conceptualization-Equal; Funding acquisition-Lead; Supervision-Equal; Writing – original draft-Equal; Writing - Review & Editing-Equal. **Paula Pérez:** Conceptualization-Equal; Formal analysis-Lead; Funding acquisition-Supporting; Investigation-Equal; Supervision-Equal; Visualization-Equal; Writing – original draft-Equal; Writing – Review and Editing-Equal.

## ACKNOWLEDGEMENTS

We thank members of other research groups from the INBIRS Institute and Dr. Juan Pablo Cerliani for technical advice and support, and critical reading of the manuscript. We especially want to thank volunteers who donate their blood samples for this project. We also thank Dr. Ana L. Riveros Salvatierra (FONDEQUIP EQM160157, School of Chemical and Pharmaceutical Sciences, University of Chile), Dr. Manuel Varas-Godoy (Cancer Cell Biology Lab, CEBICEM, School of Medicine and Science, San Sebastian University, Chile), Dr. Juan Pablo Tosar and Pablo Fagúndez (Analytical Biochemistry Unit, Sciences School, UDELAR, Uruguay) for their assistance on particle analysis determinations. This publication was supported by the United States National Institutes of Health, National Institute on Drug Abuse Grant No. R01DA040385 to KWW and MO; by the University of Miami's Centre for AIDS Research/Sylvester Comprehensive Cancer Centre – Argentina Consortium for AIDS-Malignancies Grant No U54-CA0221208 to PSP; and by the Argentinean National Agency for Science and Technology Promotion (ANPCYT) under Grants No. PICT 2015-0658, PICT-2018-02202 and PICT-2019-02506 to MO and Grant No. PICT 2019-00907 to PSP.

## CONFLICT OF INTEREST

The authors report no conflicts of interest.

## REFERENCES

- Atay, S., Gercel-Taylor, C., & Taylor, D. D. (2011). Human trophoblast-derived exosomal fibronectin induces pro-inflammatory IL-1 $\beta$  production by macrophages. *American Journal of Reproductive Immunology*, 66(4), 259–269.
- Baluk, P., Hirata, A., Thurston, G., Fujiwara, T., Neal, C. R., Michel, C. C., & McDonald, D. M. (1997). Endothelial gaps: Time course of formation and closure in inflamed venules of rats. *American Journal of Physiology*, 272(1 Pt 1), L155–L170.
- Bannoud, N., García, P. A., Gambarte-Tudela, J., Sundblad, V., Cagnoni, A. J., Bach, C. A., Pérez Saez, J. M., Blidner, A. G., Maller, S. M., Mariño, K. V., Salatino, M., Cerliani, J. P., Rabinovich, G. A., & Croci, D. O. (2022). Untangling galectin-mediated circuits that control hypoxia-driven angiogenesis. *Methods in Molecular Biology*, 2442, 635–653. [https://doi.org/10.1007/978-1-0716-2055-7\\_34](https://doi.org/10.1007/978-1-0716-2055-7_34)
- Barrès, C., Blanc, L., Bette-Bobillo, P., André, S., Mamoun, R., Gabius, H.-J., & Vidal, M. (2010). Galectin-5 is bound onto the surface of rat reticulocyte exosomes and modulates vesicle uptake by macrophages. *Blood*, 115(3), 696–705.
- Basil, M. C., & Levy, B. D. (2016). Specialized pro-resolving mediators: Endogenous regulators of infection and inflammation. *Nature Reviews Immunology*, 16(1), 51–67.
- Bei, Y., Xu, T., Lv, D., Yu, P., Xu, J., Che, L., Das, A., Tigges, J., Toxavidis, V., Ghiran, I., Shah, R., Li, Y., Zhang, Y., Das, S., & Xiao, J. (2017). Exercise-induced circulating extracellular vesicles protect against cardiac ischemia-reperfusion injury. *Basic Research in Cardiology*, 112(4), 38.
- Bernard, M. A., Zhao, H., Yue, S. C., Anandaiah, A., Koziel, H., & Tachado, S. D. (2014). Novel HIV-1 MiRNAs stimulate TNF $\alpha$  release in human macrophages via TLR8 signaling pathway. *PLoS ONE*, 9(9), e106006.
- Boilard, E. (2018). Extracellular vesicles and their content in bioactive lipid mediators: More than a sack of microRNA. *Journal of Lipid Research*, 59(11), 2037–2046.
- Böing, A. N., Der, P. E. V., Grootemaat, A. E., a, C. F., Sturk, A., & Nieuwland, R. (2014). Single-step isolation of extracellular vesicles from plasma by size-exclusion chromatography. *Int Meet ISEV Rotterdam*, 3, 118.
- Bonjoch, L., Casas, V., Carrascal, M., & Closa, D. (2016). Involvement of exosomes in lung inflammation associated with experimental acute pancreatitis. *Journal of Pathology*, 240(2), 235–245.
- Brahmer, A., Neuberger, E., Esch-Heisser, L., Haller, N., Jorgensen, M. M., Baek, R., Möbius, W., Simon, P., & Krämer-Albers, E.-M. (2019). Platelets, endothelial cells and leukocytes contribute to the exercise-triggered release of extracellular vesicles into the circulation. *Journal of Extracellular Vesicles*, 8(1), 1615820.
- Brusini, R., Varna, M., & Couvreur, P. (2020). Advanced nanomedicines for the treatment of inflammatory diseases. *Advanced Drug Delivery Reviews*, 15, 161–178.
- Buzas, E. I., György, B., Nagy, G., Falus, A., & Gay, S. (2014). Emerging role of extracellular vesicles in inflammatory diseases. *Nature Reviews Rheumatology*, 10(6), 356–364. Available from: <https://doi.org/10.1038/nrrheum.2014.19>
- Chen, L., Chen, R., Kemper, S., Cong, M., You, H., & Brigstock, D. R. (2018). Therapeutic effects of serum extracellular vesicles in liver fibrosis. *Journal of Extracellular Vesicles*, 7(1), 1461505.
- Chettimada, S., Lorenz, D. R., Misra, V., Dillon, S. T., Reeves, R. K., Manickam, C., Morgello, S., Kirk, G. D., Mehta, S. H., & Gabuzda, D. (2018). Exosome markers associated with immune activation and oxidative stress in HIV patients on antiretroviral therapy. *Scientific Reports*, 8, 7227.
- Cho, W., & Choe, J. (2020). Prostaglandin E2 stimulates COX-2 expression via mitogen-activated protein kinase p38 but not ERK in human follicular dendritic cell-like cells. *BMC Immunology [Electronic Resource]*, 21(1), 20.
- Colombo, M., Raposo, G., & Théry, C. (2014). Biogenesis, secretion, and intercellular interactions of exosomes and other extracellular vesicles. *Annual Review of Cell and Developmental Biology*, 30(1), 255–289.
- Cooks, T., Pateras, I. S., Jenkins, L. M., Patel, K. M., Robles, A. I., Morris, J., Forshew, T., Appella, E., Gorgoulis, V. G., & Harris, C. C. (2018). Mutant p53 cancers reprogram macrophages to tumor supporting macrophages via exosomal miR-1246. *Nature Communications*, 9(1), 771.
- Crawford, N. (1971). The presence of contractile proteins in platelet microparticles isolated from human and animal platelet-free plasma. *British Journal of Haematology*, 21(1), 53–69.

- Dalli, J., & Serhan, C. N. (2012). Specific lipid mediator signatures of human phagocytes: Microparticles stimulate macrophage efferocytosis and pro-resolving mediators. *Blood*, *120*(15), e60–e72.
- De Boer, C., & Davies, N. H. (2022). Blood derived extracellular vesicles as regenerative medicine therapeutics. *Biochimie*, *196*, 203–215.
- Deng, Z.-B., Zhuang, X., Ju, S., Xiang, X., Mu, J., Liu, Y., Jiang, H., Zhang, L., Mobley, J., McClain, C., Feng, W., Grizzle, W., Yan, J., Miller, D., Kronenberg, M., & Zhang, H.-G. (2013). Exosome-like nanoparticles from intestinal mucosal cells carry prostaglandin E2 and suppress activation of liver NKT cells. *Journal of Immunology*, *190*(7), 3579–3589.
- Donzelli, J., Proestler, E., Riedel, A., Nevermann, S., Hertel, B., Guenther, A., Gattenlöhner, S., Savai, R., Larsson, K., & Saul, M. J. (2021). Small extracellular vesicle-derived miR-574-5p regulates PGE2-biosynthesis via TLR7/8 in lung cancer. *Journal of Extracellular Vesicles*, *10*(12), 12143.
- Duchez, A.-C., Boudreau, L. H., Naika, G. S., Bollinger, J., Belleannée, C., Cloutier, N., Laffont, B., Mendoza-Villaruel, R. E., Lévesque, T., Rollet-Labelle, E., Rousseau, M., Allaëys, I., Tremblay, J. J., Poubelle, P. E., Lambeau, G., Pouliot, M., Provost, P., Soulet, D., Gelb, M. H., & Boilard, E. (2015). Platelet microparticles are internalized in neutrophils via the concerted activity of 12-lipoxygenase and secreted phospholipase A2-IIA. *PNAS*, *112*(27), E3564–73.
- Duette, G., Pereyra Gerber, P., Rubione, J., Perez, P. S., Landay, A. L., Crowe, S. M., Liao, Z., Witwer, K. W., Holgado, M. P., Salido, J., Geffner, J., Sued, O., Palmer, C. S., & Ostrowski, M. (2018). Induction of HIF-1 $\alpha$  by HIV-1 infection in CD4+ T cells promotes viral replication and drives extracellular vesicle-mediated inflammation. *MBio*, *9*(5), 1–21. Available from: <https://doi.org/10.1128/mBio.00757-18>
- Escobar, C., Kao, C.-Y., Das, S., & Papoutsakis, E. T. (2020). Human megakaryocytic microparticles induce de novo platelet biogenesis in a wild-type murine model. *Blood Advances*, *4*(5), 804–814.
- Feng, D., Zhao, W.-L., Ye, Y.-Y., Bai, X.-C., Liu, R.-Q., Chang, L.-F., Zhou, Q., & Sui, S.-F. (2010). Cellular internalization of exosomes occurs through phagocytosis. *Traffic (Copenhagen, Denmark)*, *11*(5), 675–687.
- Freire-De-Lima, C. G., Xiao, Yi Q., Gardai, S. J., Bratton, D. L., Schiemann, W. P., & Henson, P. M. (2006). Apoptotic cells, through transforming growth factor- $\beta$ , coordinately induce anti-inflammatory and suppress pro-inflammatory eicosanoid and NO synthesis in murine macrophages. *Journal of Biological Chemistry*, *281*(50), 38376–38384.
- French, S. L., Butov, K. R., Allaëys, I., Canas, J., Morad, G., Davenport, P., Laroche, A., Trubina, N. M., Italiano, J. E., Moses, M. A., Sola-Visner, M., Boilard, E., Pantelev, M. A., & Machlus, K. R. (2020). Platelet-derived extracellular vesicles infiltrate and modify the bone marrow during inflammation. *Blood Advances*, *4*(13), 3011–3023. <https://doi.org/10.1182/bloodadvances.2020001758>
- Frühbeis, C., Helmig, S., Tug, S., Simon, P., & Krämer-Albers, E.-M. (2015). Physical exercise induces rapid release of small extracellular vesicles into the circulation. *Journal of Extracellular Vesicles*, *4*(1), 28239.
- Fujino, H., Salvi, S., & Regan, J. W. (2005). Differential regulation of phosphorylation of the cAMP response element-binding protein after activation of EP2 and EP4 prostanoid receptors by prostaglandin E2. *Molecular Pharmacology*, *68*(1), 251–259.
- George, J., Thoi, L., Mcmanus, L., & Reimann, T. (1982). Isolation of human platelet membrane microparticles from plasma and serum. *Blood*, *60*(4), 834–840.
- Gill, S. K., Yao, Y., Kay, L. J., Bewley, M. A., Marriott, H. M., & Peachell, P. T. (2016). The anti-inflammatory effects of PGE2 on human lung macrophages are mediated by the EP4 receptor. *British Journal of Pharmacology*, 3099–3109.
- Grange, C., Tapparo, M., Bruno, S., Chatterjee, D., Quesenberry, P. J., Tetta, C., & Camussi, G. (2014). Biodistribution of mesenchymal stem cell-derived extracellular vesicles in a model of acute kidney injury monitored by optical imaging. *International Journal of Molecular Medicine*, *33*(5), 1055–1063.
- Hamidzadeh, K., Belew, A. T., El-Sayed, N. M., & Mosser, D. M. (2020). The transition of M-CSF – derived human macrophages to a growth-promoting phenotype. *Blood Advances*, *4*(21), 5460–5472.
- Hamidzadeh, K., Christensen, S. M., Dalby, E., Chandrasekaran, P., & Mosser, D. M. (2017). Macrophages and the recovery from acute and chronic inflammation. *Annual Review of Physiology*, *79*, 567–592.
- Hirata, A., Baluk, P., Fujiwara, T., & McDonald, D. M. (1995). Location of focal silver staining at endothelial gaps in inflamed venules examined by scanning electron microscopy. *American Journal of Physiology*, *269*(3 Pt 1), L403–18.
- Honda, A., Sugimoto, Y., Namba, T., Watabe, A., Irie, A., Negishi, M., Narumiya, S., & Ichikawa, A. (1993). Cloning and expression of a cDNA for mouse prostaglandin E receptor EP2 subtype. *Journal of Biological Chemistry*, *268*(11), 7759–7762.
- Hoshino, A., Kim, H. S., Bojmar, L., Gyan, K. E., Cioffi, M., Hernandez, J., Zambirinis, C. P., Rodrigues, G., Molina, H., Heissel, S., Mark, M. T., Steiner, L., Benito-Martin, A., Lucotti, S., Di Giannatale, A., Offer, K., Nakajima, M., Williams, C., Nogués, L., ... Lyden, D. (2020). Extracellular vesicle and particle biomarkers define multiple human cancers. *Cell*, *182*(4), 1044–1061.e18.
- Hou, Z., Qin, X., Hu, Y., Zhang, X., Li, G., Wu, J., Li, J., Sha, J., Chen, J., Xia, J., Wang, L., & Gao, F. (2019). Longterm exercise-derived exosomal miR-342-5p: A novel exerkine for cardioprotection. *Circulation Research*, *124*(9), 1386–1400.
- Hsu, H.-H., Lin, Y.-M., Shen, C.-Y., Shibu, M., Li, S.-Y., Chang, S.-H., Lin, C.-C., Chen, R.-J., Viswanadha, V., Shih, H.-N., & Huang, C.-Y. (2017). Prostaglandin E2-induced COX-2 expressions via EP2 and EP4 signaling pathways in human LoVo colon cancer cells. *International Journal of Molecular Sciences*, *18*(6), 1132.
- Hu, Q., Lyon, C. J., Fletcher, J. K., Tang, W., Wan, M., & Hu, T. Y. (2021). Extracellular vesicle activities regulating macrophage- and tissue-mediated injury and repair responses. *Acta Pharmaceutica Sinica B*, *11*(6), 1493–1512. <https://doi.org/10.1016/j.apsb.2020.12.014>
- Hyenne, V., Ghoroghi, S., Collot, M., Bons, J., Follain, G., Harlepp, S., Mary, B., Bauer, J., Mercier, L., Busnelli, I., Lefebvre, O., Fekonja, N., Garcia-Leon, M. J., Machado, P., Delalande, F., López, A. A., Silva, S. G., Verweij, F. J., Van Niel, G., ... Goetz, J. G. (2019). Studying the fate of tumor extracellular vesicles at high spatiotemporal resolution using the Zebrafish embryo. *Developmental Cell*, *48*(4), 554–572.e7.
- Hyvärinen, K., Holopainen, M., Skirdenko, V., Ruhanen, H., Lehenkari, P., Korhonen, M., Käkälä, R., Laitinen, S., & Kerkele, E. (2018). Mesenchymal stromal cells and their extracellular vesicles enhance the anti-inflammatory phenotype of regulatory macrophages by downregulating the production of interleukin (IL)-23 and IL-22. *Frontiers in Immunology*, *9*, 771.
- Imai, T., Takahashi, Y., Nishikawa, M., Kato, K., Morishita, M., Yamashita, T., Matsumoto, A., Charoenviriyakul, C., & Takakura, Y. (2015). Macrophage-dependent clearance of systemically administered B16BL6-derived exosomes from the blood circulation in mice. *Journal of Extracellular Vesicles*, *4*(1), 26238.
- Just, J., Yan, Y., Farup, J., Sieljacks, P., Sloth, M., Venø, M., Gu, T., De Paoli, F. V., Nyengaard, J. R., Bæk, R., Jørgensen, M. M., Kjems, J., Vissing, K., & Drasbek, K. R. (2020). Blood flow-restricted resistance exercise alters the surface profile, miRNA cargo and functional impact of circulating extracellular vesicles. *Scientific Reports*, *10*(1), 1–13.
- Kalani, M. Y. S., Alsop, E., Meechoovet, B., Beecroft, T., Agrawal, K., Whitsett, T. G., Huentelman, M. J., Spetzler, R. F., Nakaji, P., Kim, S., & Van Keuren-Jensen, K. (2020). Extracellular microRNAs in blood differentiate between ischaemic and haemorrhagic stroke subtypes. *Journal of Extracellular Vesicles*, *9*(1), 1713540.
- Kalinski, P. (2012). Regulation of immune responses by prostaglandin E2. *Journal of Immunology*, *188*(1), 21–28.
- Karimi, N., Cvjetkovic, A., Jang, Su C., Crescitelli, R., Hosseinpour Feizi, M. A., Nieuwland, R., Lötval, J., & Lässer, C. (2018). Detailed analysis of the plasma extracellular vesicle proteome after separation from lipoproteins. *Cellular and Molecular Life Sciences*, *75*(15), 2873–2886.
- Karimi, N., Dalirfardouei, R., Dias, T., Lötval, J., & Lässer, C. (2022). Tetraspanins distinguish separate extracellular vesicle subpopulations in human serum and plasma-Contributions of platelet extracellular vesicles in plasma samples. *Journal of Extracellular Vesicles*, *11*, 12213.



- Khan, S., Bennit, H. F., Turay, D., Perez, M., Mirshahidi, S., Yuan, Y., & Wall, N. R. (2014). Early diagnostic value of survivin and its alternative splice variants in breast cancer. *BMC Cancer*, *14*, 176.
- Kuroda, E., & Yamashita, U. (2022). Mechanisms of enhanced macrophage-mediated prostaglandin E2 production and its suppressive role in Th1 activation in Th2-dominant BALB/c mice. *Journal of Immunology*, *170*, 757–764.
- Linton, S. S., Abraham, T., Liao, J., Clawson, G. A., Butler, P. J., Fox, T., Kester, M., & Matters, G. L. (2018). Tumor-promoting effects of pancreatic cancer cell exosomes on THP-1-derived macrophages. *PLoS ONE*, *13*(11), 1–20.
- Liu, R., Tang, A., Wang, X., Chen, X., Zhao, L., Xiao, Z., & Shen, S. (2018). Inhibition of lncRNA NEAT1 suppresses the inflammatory response in IBD by modulating the intestinal epithelial barrier and by exosome-mediated polarization of macrophages. *International Journal of Molecular Medicine*, *42*(5), 2903–2913.
- Liu, Y., Sun, D., Fan, Q., Ma, Q., Dong, Z., Tao, W., Tao, H., Liu, Z., & Wang, C. (2020). The enhanced permeability and retention effect based nanomedicine at the site of injury. *Nano Research*, *13*(2), 564–569. <https://doi.org/10.1007/s12274-020-2655-6>
- Locati, M., Curtale, G., & Mantovani, A. (2020). Diversity, mechanisms, and significance of macrophage plasticity. *Annual Review of Pathology: Mechanisms of Disease*, *15*, 123–147.
- Luan, B., Yoon, Y.-S., Le Lay, J., Kaestner, K. H., Hedrick, S., & Montminy, M. (2015). CREB pathway links PGE2 signaling with macrophage polarization. *PNAS*, *112*(51), 15642–15647.
- Mackenzie, K. F., Clark, K., Naqvi, S., Mcguire, V. A., Nöhren, G., Kristariyanto, Y., Van Den Bosch, M., Mudaliar, M., Mccarthy, P. C., Pattison, M. J., Pedrioli, P. G. A., Barton, G. J., Toth, R., Prescott, A., & Arthur, J. S. C. (2013). PGE(2) induces macrophage IL-10 production and a regulatory-like phenotype via a protein kinase A-SIK-CRTC3 pathway. *Journal of Immunology*, *190*(2), 565–577.
- Mastronardi, M. L., Mostefai, H. A., Mezziani, F., Martínez, M. C., Asfar, P., & Andriantsitohaina, R. (2011). Circulating microparticles from septic shock patients exert differential tissue expression of enzymes related to inflammation and oxidative stress. *Critical Care Medicine*, *39*(7), 1739–1748.
- Mosser, D. M., & Edwards, J. P. (2008). Exploring the full spectrum of macrophage activation. *Nature Reviews Immunology*, *8*(12), 958–969. <https://doi.org/10.1038/nri2448>
- Murakami, M., Naraba, H., Tanioka, T., Semmyo, N., Nakatani, Y., Kojima, F., Ikeda, T., Fueki, M., Ueno, A., Oh-Ishi, S., & Kudo, I. (2000). Regulation of prostaglandin E2 biosynthesis by inducible membrane-associated prostaglandin E2 synthase that acts in concert with cyclooxygenase-2. *Journal of Biological Chemistry*, *275*(42), 32783–32792.
- Murray, P. J. (2017). Macrophage polarization. *Annual Review of Physiology*, *79*, 541–566.
- Na, Y. R., Jung, D., Yoon, B. R., Lee, W. W., & Seok, S. H. (2015). Endogenous prostaglandin E2 potentiates anti-inflammatory phenotype of macrophage through the CREB-C/EBP- $\beta$  cascade. *European Journal of Immunology*, *45*(9), 2661–2671.
- Nakayama, T., Mutsuga, N., Yao, L., & Tosato, G. (2006). Prostaglandin E2 promotes degranulation-independent release of MCP-1 from mast cells. *Journal of Leukocyte Biology*, *79*(1), 95–104.
- Nakazaki, M., Morita, T., Lankford, K. L., Askenase, P. W., & Kocsis, J. D. (2021). Small extracellular vesicles released by infused mesenchymal stromal cells target M2 macrophages and promote TGF- $\beta$  upregulation, microvascular stabilization and functional recovery in a rodent model of severe spinal cord injury. *Journal of Extracellular Vesicles*, *10*(1), e12137.
- Nathan, C., & Ding, A. (2010). Nonresolving inflammation. *Cell*, *140*(6), 871–882.
- Oliveira, G. P., Porto, W. F., Palu, C. C., Pereira, L. M., Petriz, B., Almeida, J. A., Viana, J., Filho, N. N. A., Franco, O. L., & Pereira, R. W. (2018). Effects of acute aerobic exercise on rats serum extracellular vesicles diameter, concentration and small RNAs content. *Frontiers in Physiology*, *9*(MAY), 1–11.
- Ostalecki, C., Wittki, S., Lee, J.-H., Geist, M. M., Tibroni, N., Harrer, T., Schuler, G., Fackler, O. T., & Baur, A. S. (2016). HIV Nef- and Notch1-dependent endocytosis of ADAM17 induces vesicular TNF secretion in chronic HIV infection. *EBioMedicine*, *13*, 294–304.
- Otahal, A., Kramer, K., Kuten-Pella, O., Moser, L. B., Neubauer, M., Lacza, Z., Nehrer, S., & De Luna, A. (2021). Effects of extracellular vesicles from blood-derived products on osteoarthritic chondrocytes within an inflammation model. *International Journal of Molecular Sciences*, *22*(13), 1–15.
- Park, J. E., Dutta, B., Tse, S. W., Gupta, N., Tan, C. F., Low, J. K., Yeoh, K. W., Kon, O. I., Tam, J. P., & Sze, S. K. (2019). Hypoxia-induced tumor exosomes promote M2-like macrophage polarization of infiltrating myeloid cells and microRNA-mediated metabolic shift. *Oncogene*, *38*(26), 5158–5173.
- Pérez, P. S., Romaniuk, M. A., Duette, G. A., Zhao, Z., Huang, Y., Martin-Jaular, L., Witwer, K. W., Théry, C., & Ostrowski, M. (2019). Extracellular vesicles and chronic inflammation during HIV infection. *Journal of Extracellular Vesicles*, *8*(1), 1687275.
- Phipps, R. P., Stein, S. H., & Roper, R. L. (1991). A new view of prostaglandin E regulation of the immune response. *Immunology Today*, *12*(10), 349–352.
- Plebanek, M. P., Angeloni, N. L., Vinokour, E., Li, J., Henkin, A., Martinez-Marin, D., Filleur, S., Bhowmick, R., Henkin, J., Miller, S. D., Ifergan, I., Lee, Y., Osman, I., Thaxton, C. S., & Volpert, O. V. (2017). Pre-metastatic cancer exosomes induce immune surveillance by patrolling monocytes at the metastatic niche. *Nature Communications*, *8*, 1319.
- Qian, M., Wang, S., Guo, X., Wang, J., Zhang, Z., Qiu, W., Gao, X., Chen, Z., Xu, J., Zhao, R., Xue, H., & Li, G. (2020). Hypoxic glioma-derived exosomes deliver microRNA-1246 to induce M2 macrophage polarization by targeting TERF2IP via the STAT3 and NF- $\kappa$ B pathways. *Oncogene*, *39*(2), 428–442.
- Quinn, J. F., Patel, T., Wong, D., Das, S., Freedman, J. E., Laurent, L. C., Carter, B. S., Hochberg, F., Keuren-Jensen, K. V., Huentelman, M., Spetzler, R., S Kalani, M. Y., Arango, J., Adelson, P. D., Weiner, H. L., Gandhi, R., Goilav, B., Putterman, C., & Saugstad, J. A. (2015). Extracellular RNAs: Development as biomarkers of human disease. *Journal of Extracellular Vesicles*, *4*(1), 27495.
- Rabinowitz, G., Gerçel-Taylor, C., Day, J. M., Taylor, D. D., & Kloecker, G. H. (2009). Exosomal microRNA: A diagnostic marker for lung cancer. *Clinical Lung Cancer*, *10*(1), 42–46.
- Regan, J. W., Bailey, T. J., Pepperl, D. J., Pierce, K. L., Bogardus, A. M., Donello, J. E., Fairbairn, C. E., Kedzie, K. M., Woodward, D. F., & Gil, D. W. (1994). Cloning of a novel human prostaglandin receptor with characteristics of the pharmacologically defined EP2 subtype. *Molecular Pharmacology*, *46*(2), 213–220.
- Rossaint, J., Kühne, K., Skupski, J., Van Aken, H., Looney, M. R., Hidalgo, A., & Zarbock, A. (2016). Directed transport of neutrophil-derived extracellular vesicles enables platelet-mediated innate immune response. *Nature Communications*, *7*, 13464.
- Ruffell, D., Mourkioti, F., Gambardella, A., Kirstetter, P., Lopez, R. G., Rosenthal, N., & Nerlov, C. (2009). A CREB-C/EBP $\beta$  cascade induces M2 macrophage-specific gene expression and promotes muscle injury repair. *PNAS*, *106*(41), 17475–17480.
- Scher, J. U., & Pillinger, M. H. (2009). The anti-inflammatory effects of prostaglandins. *The Journal of Investigative Medicine*, *57*(6), 703–709.
- Serhan, C. N., & Levy, B. (2003). Success of prostaglandin E2 in structure-function is a challenge for structure-based therapeutics. *PNAS*, *100*(15), 8609–8611.
- Serhan, C. N., & Savill, J. (2005). Resolution of inflammation: The beginning programs the end. *Nature Immunology*, *6*(12), 1191–1197.
- Shaywitz, A. J., & Greenberg, M. E. (1999). CREB: A stimulus-induced transcription factor activated by a diverse array of extracellular signals. *Annual Review of Biochemistry*, *68*, 821–861.

- Sokolowska, M., Chen, L.-Y., Liu, Y., Martinez-Anton, A., Qi, H.-Y., Logun, C., Alsaaty, S., Park, Y. H., Kastner, D. L., Chae, J. J., & Shelhamer, J. H. (2015). Prostaglandin E2 inhibits NLRP3 inflammasome activation through EP4 receptor and intracellular cyclic AMP in human macrophages. *Journal of Immunology*, *194*(11), 5472–5487.
- Subra, C., Grand, D., Laulagnier, K., Stella, A., Lambeau, G., Paillasse, M., De Medina, P., Monsarrat, B., Perret, B., Silvente-Poirot, S., Poirot, M., & Record, M. (2010). Exosomes account for vesicle-mediated transcellular transport of activatable phospholipases and prostaglandins. *Journal of Lipid Research*, *51*(8), 2105–2120.
- Suda, M., Tanaka, K., Yasoda, A., Natsui, K., Sakuma, Y., Tanaka, I., Ushikubi, F., Narumiya, S., & Nakao, K. (1998). Prostaglandin E2 (PGE2) autoamplifies its production through EPI subtype of PGE receptor in mouse osteoblastic MC3T3-E1 cells. *Calcified Tissue International*, *62*(4), 327–331.
- Tai, H.-H., Ensor, C. M., Tong, M., Zhou, H., & Yan, F. (2002). Prostaglandin catabolizing enzymes. *Prostaglandins & Other Lipid Mediators*, *68–69*, 483–493.
- Takayama, K., García-Cardena, G., Sukhova, G. K., Comander, J., Gimbrone, M. A., & Libby, P. (2002). Prostaglandin E2 suppresses chemokine production in human macrophages through the EP4 receptor. *Journal of Biological Chemistry*, *277*(46), 44147–44154.
- Taylor, D. D., & Gercel-Taylor, C. (2008). MicroRNA signatures of tumor-derived exosomes as diagnostic biomarkers of ovarian cancer. *Gynecologic Oncology*, *110*(1), 13–21.
- Théry, C., Ostrowski, M., & Segura, E. (2009). Membrane vesicles as conveyors of immune responses. *Nature Reviews Immunology*, *9*(8), 581–593.
- Théry, C., Witwer, K. W., Aikawa, E., Alcaraz, M. J., Anderson, J. D., Andriantsitohaina, R., Antoniou, A., Arab, T., Archer, F., Atkin-Smith, G. K., Ayre, D. C., Bach, J.-M., Bachurski, D., Baharvand, H., Balaj, L., Baldacchino, S., Bauer, N. N., Baxter, A. A., Bebawy, M., ... Zuba-Surma, E. K. (2018). Minimal information for studies of extracellular vesicles 2018 (MISEV2018): A position statement of the international society for extracellular vesicles and update of the MISEV2014 guidelines. *Journal of Extracellular Vesicles*, *7*(1), 1535750.
- Tkach, M., Thalmensi, J., Timperi, E., Gueguen, P., Névo, N., Grisard, E., Sirven, P., Coccozza, F., Gouronnet, A., Martin-Jaular, L., Jouve, M., Delisle, F., Manel, N., Rookhuizen, D. C., Guerin, C. L., Soumelis, V., Romano, E., Segura, E., & Théry, C. (2022). Extracellular vesicles from triple negative breast cancer promote pro-inflammatory macrophages associated with better clinical outcome. *PNAS*, *119*(17), 1–12.
- Vacchi, E., Burrello, J., Di Silvestre, D., Burrello, A., Bolis, S., Mauri, P., Vassalli, G., Cereda, C. W., Farina, C., Barile, L., Kaelin-Lang, A., & Melli, G. (2020). Immune profiling of plasma-derived extracellular vesicles identifies Parkinson disease. *Neurology: Neuroimmunology and NeuroInflammation*, *7*(6), e866.
- Van Deun, J., Mestdagh, P., Agostinis, P., Akay, Ö., Anand, S., Anckaert, J., Martinez, Z. A., Baetens, T., Beghein, E., Bertier, L., Berx, G., Boere, J., Boukouris, S., Bremer, M., Buschmann, D., Byrd, J. B., Casert, C., Cheng, L., ... Hendrix, A. (2017). EV-TRACK: Transparent reporting and centralizing knowledge in extracellular vesicle research. *Nature Methods*, *14*, 228–232.
- Vannella, K. M., & Wynn, T. A. (2017). Mechanisms of organ injury and repair by macrophages. *Annual Review of Physiology*, *79*(November), 593–617.
- Verweij, F. J., Revenu, C., Arras, G., Dingli, F., Loew, D., Pegtel, D. M., Follain, G., Allio, G., Goetz, J. G., Zimmermann, P., Herbomel, P., Del Bene, F., Raposo, G., & Van Niel, G. (2019). Live tracking of inter-organ communication by endogenous exosomes in vivo. *Developmental Cell*, *48*(4), 573–589.e4.e4.
- Wang, X. S., & Lau, H. Y. A. (2006). Prostaglandin E potentiates the immunologically stimulated histamine release from human peripheral blood-derived mast cells through EPI/EP3 receptors. *Allergy*, *61*(4), 503–506.
- Weller, C. L., Collington, S. J., Hartnell, A., Conroy, D. M., Kaise, T., Barker, J. E., Wilson, M. S., Taylor, G. W., Jose, P. J., & Williams, T. J. (2007). Chemotactic action of prostaglandin E2 on mouse mast cells acting via the PGE2 receptor 3. *PNAS*, *104*(28), 11712–11717.
- Wen, A. Y., Sakamoto, K. M., & Miller, L. S. (2010). The role of the transcription factor CREB in immune function. *Journal of Immunology*, *185*(11), 6413–6419.
- Wong, W.-Y., Lee, M. M.-L., Chan, B. D., Kam, R. K.-T., Zhang, G., Lu, Ai-P., & Tai, W. C.-S. (2016). Proteomic profiling of dextran sulfate sodium induced acute ulcerative colitis mice serum exosomes and their immunomodulatory impact on macrophages. *Proteomics*, *16*(7), 1131–1145.
- Wu, J., Piao, Y., Liu, Q., & Yang, X. (2021). Platelet-rich plasma-derived extracellular vesicles: A superior alternative in regenerative medicine? *Cell Proliferation*, *54*(12), 1–13.
- Xiang, X., Poliakov, A., Liu, C., Liu, Y., Deng, Z.-B., Wang, J., Cheng, Z., Shah, S. V., Wang, G.-J., Zhang, L., Grizzle, W. E., Mobley, J., & Zhang, H.-G. (2009). Induction of myeloid-derived suppressor cells by tumor exosomes. *International Journal of Cancer*, *124*(11), 2621–2633.
- Y, Y., & Chadee, K. (1998). Prostaglandin E2 stimulates IL-8 gene expression in human colonic epithelial cells by a posttranscriptional mechanism. *Journal of Immunology*, *161*(7), 3746–3752.
- Yan, F., Zhong, Z., Wang, Y., Feng, Y., Mei, Z., Li, H., Chen, X., Cai, L., & Li, C. (2020). Exosome-based biomimetic nanoparticles targeted to inflamed joints for enhanced treatment of rheumatoid arthritis. *Journal of Nanobiotechnology*, *18*(1), 115.
- Yoshida, M., Satoh, A., Lin, J. B., Mills, K. F., Sasaki, Y., Rensing, N., Wong, M., Apte, R. S., & Imai, S.-I. (2019). Extracellular vesicle-contained eNAMPT delays aging and extends lifespan in mice. *Cell Metabolism*, *30*(2), 329–342.e5.e5.
- Yuyama, K., Sun, H., Mitsutake, S., & Igarashi, Y. (2012). Sphingolipid-modulated exosome secretion promotes clearance of amyloid- $\beta$  by microglia. *Journal of Biological Chemistry*, *287*(14), 10977–10989. <https://doi.org/10.1074/jbc.M111.324616>

## SUPPORTING INFORMATION

Additional supporting information can be found online in the Supporting Information section at the end of this article.

**How to cite this article:** Adamczyk, A. M., Leicaj, M. L., Fabiano, M. P., Cabrerizo, G., Bannoud, N., Croci, D. O., Witwer, K. W., Remes Lenicov, F., Ostrowski, M., & Pérez, P. S. (2023). Extracellular vesicles from human plasma dampen inflammation and promote tissue repair functions in macrophages. *Journal of Extracellular Vesicles*, *12*, e12331. <https://doi.org/10.1002/jev2.12331>